NPS ARCHIVE
1966
BRUMWELL, R.

RADIOISOTOPE TRACING OF METALLIC DEPOSITS NEAR A COAXIAL PLASMA GUN EXHAUST

ROBERT K. BRUMWELL

DUDLEY KNOX LIBRARY
NAVAL POSTGRADUATE SCHOOL
MONTEREY, CA 93943-5101

...STGRADUATE SCHOOL
MONTEREY, CALIF. 93940

This document has been approved for public
release and sale; its distribution is unlimited.

RADIOISOTOPE TRACING OF METALLIC DEPOSITS NEAR A COAXIAL PLASMA GUN EXHAUST

by

Robert K. Brumwell
Lieutenant, United States Navy
B.S., North Dakota State University, 1956

Submitted in partial fulfillment
for the degree of

AERONAUTICAL ENGINEER

from the

UNITED STATES NAVAL POSTGRADUATE SCHOOL
May 1966

NPS ARCHIVE
1966
BRUMWELL, R.
Thesis
B82637
c.1

ABSTRACT

A coaxial plasma accelerator system was constructed by LT R. K. Brumwell, USN at the United States Naval Postgraduate School for the purpose of producing a high velocity plasma slug. Experiments were performed in an evacuated chamber. Operating procedures were established for the apparatus and calibration tests were performed which demonstrated reproducibility of accelerator discharges made under given conditions.

Use of a radioisotope tracer technique to measure the deposition of a metallic plasma on a cold wall was then investigated. A series of tests was conducted which demonstrates the feasibility of this tracer method for determination of mass condensation on walls surrounding a high velocity plasma slug.

DUDLEY KNOX LIBRARY
NAVAL POSTGRADUATE SCHOOL
MONTEREY, CA 93943-5101

TABLE OF CONTENTS

Section		Page
1.	Introduction	9
2.	Plasma Accelerator Theory	13
3.	Accelerator System Experimental Apparatus	16
4.	Plasma Gun Experimental Firing Procedure	22
5.	Tracer Analysis Theory	23
6.	Tracer Analysis Equipment	26
7.	Tracer Analysis Procedure	27
8.	Results and Discussion	31
9.	Conclusions	36
10.	Suggestions for Further Investigation	37
11.	Bibliography	38
Appendix		
I.	Procedures Checklists	76
II.	Capacitor Voltmeter Calibration	80
III.	Image Converter Camera Calibration	84
IV.	Preparation of Control Sample Disk	86

LIST OF TABLES

Table		Page
I	Plasma Velocity Measurement	40
II	Plasma Velocity	41
III	Tracer Results Run 19L	42
IV	Tracer Results Runs 19R and 17C	43

LIST OF ILLUSTRATIONS

Figure		Page
1.	Three Accelerators	44
2.	Accelerator System	45
3.	Accelerator Detail	46
4.	Disassembled Gun	47
5.	Assembled Gun	48
6.	Capacitor and Ignitions	49
7.	Ignition Pulser	50
8.	Capacitor Discharge Trigger	51
9.	A. Flow Switch	52
	B. Trigger Panel	52
10.	Instrumentation	53
11.	Power Control Panel	54
12.	High Voltage System	55
13.	High Volume Vacuum System and High Voltage Components	56
14.	High Vacuum System	57
15.	LN_2 System	58
16.	Vacuum Controls	59
17.	Image Converter Camera	60
18.	A. Image Converter Record	61
	B. Oscilloscope Record	61
19.	Apparatus Placement	62

20. Sample Removal 63

21. Gold 198 Gamma Radiation 64

22. Detection Apparatus 65

23. Sample Data Plot 66

24. Gold Decay 67

25. Velocity Measurement Shot 11 68

26. Velocity Measurement Shot 12 69

27. Velocity Measurement Shot 13 70

28. Velocity Measurement Shot 14 71

29. Velocity Measurement Shot 16 72

30. Velocity Measurement Shot 18 73

31. Gold Monitor Decay 74

32. Gold Deposition 75

II-1. Capacitor Voltmeter Calibration 83

1. Introduction.

The subject of magnetohydrodynamics (MHD) has its origin in speculations of certain scientists concerning the magnetism of celestial bodies. Bigelow in 1899 inferred that the sun is a huge magnet from observation of coronal plumes. [7] It was not until the last ten years however, that the study of MHD came to be of major importance. Not only is it of interest in space propulsion, but the subjects of atmospheric reentry, high speed aerodynamics, astrophysics and controlled thermonuclear power call upon MHD for insight into complex high temperature phenomena.

The basic working materials of MHD are plasmas. A plasma is an electrically conducting mixture of ions, electrons and neutral atoms with a macroscopically neutral charge. Microscopic variations may create local charge concentrations but there are enough electrons present to neutralize each positive charge.

The study of plasmas and ionized gases is complicated by the difficulty of measurement at the high temperatures, current and magnetic field densities, and velocities normally encountered. Since attempts to describe plasma dynamics analytically have been only partially successful there is a need for extended experimental research of phenomena involved.

Plasma Accelerators

Plasma acceleration devices are suitable for an ever increasing number of important and interesting applications such as low thrust, high specific impulse motors, fusion injection devices for nuclear reactors, coating guns, plasmoid generators and electromagnetic shock tubes. [5, 17] These devices

all entail the conversion of electrical energy to directed kinetic energy of a mass of plasma.

Schematics of three common magnetic plasma accelerator configurations are shown in Fig. 1. All use magnetic fields to augment the driving force on the working fluid due to rapid expansion in an arc discharge. The earliest of these is the Kolb tube. In this device the interaction of the discharge current with the field produces a force on the working fluid which is directed down the tube.

Ref. 22 gives an example of the use of the second configuration; the conical magnetic shock tube. Here the current flows from the center electrode to the ring electrode and then through the return conductor. The high current produces the magnetic field which pinches the ionized gas in the cone in such a manner as to drive it toward the ring electrode.

The third device pictured is the coaxial configuration, sometimes referred to as a magnetic annular shock tube, which was used in this work. The coaxial geometry is capable of providing a more continuous force on the gas. Additional driving force can be obtained through the use of external field coils.

Although plasma acceleration devices have been investigated by many groups in forms too numerous to mention in detail, exhaust measurements have been mostly limited to the determination of gross parameters such as thrust, total energy content, and momentum.[8, 12, 9] More detailed information on the exhaust properties is required for a better understanding of the

acceleration and flow mechanisms.

Ballistic pendulums and calorimeters have been used for exhaust energy measurements in evaluation of coaxial plasma guns as space thrustors. Gooding has shown [10] in work for NASA using such devices, that the thermal efficiency based on these exhaust measurements can be as low as 15 or 20% for an accelerator which receives 65% of initial stored capacitor energy. This low exhaust efficiency is thought to arise from radiation losses and direct loss of plasma to the electrodes.

Experiments with a coaxial plasma gun were performed by Reichenbach [19] at the Air Force Special Weapons Center. The purpose of this work was measurement of the mass distribution of a metallic plasma condensate on cold walls. Accurate quantitative results were not obtained because of difficulties with the capacitor system and the limited time spent on the project. The work described in this thesis is an attempt to investigate this phenomena of mass loss from a plasma flow using an improved capacitor and discharge system and taking advantage of the proximity of a nuclear reactor. It is felt that information of this nature will be of value in the study of thrustor applications or of plasma flows in general.

Experiment Description

The purpose of this thesis project was to set up a facility for investigation of plasma flows and then to continue the work of Reichenbach: experimental measurement of the radial transfer of mass to a cold wall from a high velocity slug of metallic plasma using radioisotope tracing.

In this experiment thin gold foils are vaporized and accelerated through coaxial electrodes into an evacuated cylindrical tube using a capacitor discharge system. After leaving the accelerator a portion of the gold vapor condenses on the inside wall of a cylindrical collector sheet which lines the tube. Mass distribution of the gold deposited on this collector is then determined using radioisotope tracing. Sample disks cut from various locations on the collector sheet are irradiated in a nuclear reactor and the amount of gold present determined from the rate of radioactive decay.

Completion of this project included:

a. Assembly of the accelerator system, including associated charging and triggering devices.

b. Design and assembly of the vacuum system, controls and vacuum measuring equipment.

c. Instrumenting the systems to insure that uniform, reproducible conditions exist for successive firings. This included high speed photographs of the plasma front to determine velocity, accurate measurement of capacitor power level, and observation of the discharge current versus time characteristics of the gun.

d. Establishing of procedures for operation of the completed system.

e. Development of a technique for using radioactive tracers to determine mass deposition on cold walls.

f. Performance of sufficient tests to reach a conclusion as to the feasibility and accuracy of this method of determining mass deposition.

This paper reports on work performed by the author during the period of August 1965 through April 1966 at the United States Naval Postgraduate School, Monterey, California. The author is indebted to Professor R. E. Reichenbach of the Aeronautics Department for his encouragement and assistance throughout the project and to Professor E. A. Milne of the Physics Department who made the Reactor Facility available and furnished technical assistance with the tracer analysis.

2. Plasma Accelerator Theory.

A plasma, being composed of charged particles and subjected to magnetic fields, must obey the laws of electromagnetics and, since it is also a gas, must also observe the laws of gas dynamics. To describe plasma dynamics, Maxwell's equations of electromagnetics are needed in addition to the normal continuity and state equations, while the energy and momentum equations are modified by the addition of ohmic heating and Lorentz force terms, respectively. The concept of magnetic pressure due to the Lorentz force is extremely important in discussions of MHD propulsion systems. If a conducting fluid, liquid metal, or ionized gas has a high electrical conductivity it is possible to creat magnetic fields strong enough to pump, confine, or accelerate it.

Fig. 1 is a schematic of a coaxial plasma accelerator. Discharge of the capacitor heats and ionizes the working material between the electrodes to form a plasma. The conducting plasma then completes the circuit between the electrodes. Current density in the plasma is denoted by $\overline{J}$. When current

flows in the center conductor a magnetic field $\overline{B}$ is induced in the vicinity of the conductor. The interaction of current and magnetic flux on an element in the field produces the Lorentz force vector $\overline{F} = \overline{J} \times \overline{B}$ per unit volume of plasma. The resulting force is seen to be directed toward the muzzle regardless of the polarity of the electrodes since a reversal of current flow direction also reverses the magnetic field. This magnetic pressure on the plasma blob pushes the gas much the same as a piston.

Two of the simplified models used in attempts to describe the motion analytically are the snowplow model and the slug model. The snowplow theory assumes that the plasma acts as a plane magnetic piston which moves through the accelerator sweeping up mass and accumulating it on the piston surface. The slug model treats the plasma as though it were a non-deformable body of constant mass. [18] Using these and other simplifying assumptions such as no resistance, constant current flow and unidirectional currents flowing in the plasma, approximate solutions have been obtained for plasma energy and velocity in terms of stored energy and circuit constants. [10] The energy partition between internal and kinetic energy, however, actually depends on the detailed behavior of the plasma and cannot be readily predicted.

It is not known, for instance, whether the electrons are the main current carriers or whether the ions play a significant role. It is hypothesized by some that the current flows through the electron sheet which in turn drags the heavier ions along some distance behind by electrostatic attraction. It

also seems reasonable that a significant number of the ions would be driven to the negative electrode be electrostatic attraction, resulting in decreased efficiency.

The magnetic pressure in the vicinity of a conductor varies as $1/r^2$ which would lead one to expect a bullet shaped plasma front. It has been found by Keck [16] that the current sheet is planar when the center conductor is the cathode and bullet shaped when the center conductor is the anode. This appears to be true with a large ratio of outer to inner conductor radius. This effect is attributed by Bostick [2] to Hall currents and plasma vortices. Hall currents are secondary current loops within the plasma caused by the potential difference between the front and rear of the sheet.

With the center conductor negative and with the Hall currents comparable in magnitude to currents in the otherwise-bullet-shaped sheet, the vector sum of currents tends to be planar. These Hall currents produce a centripetal force which deflects the plasmoid into a spiral trajectory leaving the electrodes. These radial velocity components are a cause for further losses in propulsive efficiency.

Further analytical and experimental work on the processes within the current sheet itself is necessary before this current sheet can be fully understood. A significant amount of work is presently being conducted by investigators to develop diagnostic techniques such as ion probes [1] and electrostatic particle analysers [6] to study actual particle movement within the plasma.

3. Accelerator System Experimental Apparatus.

The major portion of the work for this project was assembly and performance evaluation of the system shown schematically in Fig. 2. A detailed description of this apparatus will be presented here both as an aid in describing the experiment and as a reference for future users of the system.

Plasma Accelerator

The plasma gun was a coaxial configuration as shown in Fig. 3 with a one-inch diameter center electrode and a 1.5-inch I. D. copper barrel. The barrel was 7.5 inches in length and had four holes spaced axially for observation of the plasma before it emerged from the gun. The foil sheet, which was vaporized by the capacitor discharge and formed the plasma, was located 2.25 inches from the breech. Both electrodes were designed to come apart at the foil plane and to be reassembled without tearing the thin foil. This was accomplished in the center conductor utilizing a three piece construction with a short section above the foil acting as a nonrotating washer, and in the barrel with a flange and collar arrangement. The disassembled gun is shown in Fig. 4 with a foil nearby and in Fig. 5 ready to fire.

Gold was used as a working material because of its high conductivity, availability in thin uniform sheet, purity in commercial form, convenient radioactive half life (2.7 days), and large activation cross section. Dental gold foils .00005 inches in thickness were used. This gave 15.55 milligrams of vaporized gold.

A 2.4-inch I.D. glass cylinder was used to support a thin aluminum collector sheet upon which a portion of the plasma was deposited. Aluminum was used as a collector sheet because its small activation cross section and short radioactive half life gave minimum interference when tracing deposited gold. It was found that conventional heavy duty (1 mil) household aluminum foil was sufficiently free of long half life impurities to be used for this purpose.

A gap was left between the ends of the collector sheet as shown in Fig. 5 to permit observation of the plasma flow when the cylinder was placed over the gun. Markings on the cylinder at one-inch intervals were used to determine plasma velocity photographically. These markers were aluminum foil strips cemented to the glass with Glyptol vacuum sealant. A mark on the cylinder was used to position the lower edge of the collector sheet one inch below the gun muzzle. Two $\frac{1}{4}$-inch wide strips of thin spring steel (not shown in Fig. 5) were placed inside the sheet to insure conformity with the cylinder inner wall. These clips were located at the upper and lower edges of the collector.

Capacitor System

a. Basic discharge circuit. The capacitor was an Axel 6.4 microfarad, low inductance unit with a 2000 joule capacity at 25,000 volts. Switching was accomplished with four GL 7703 ignitrons in parallel. These ignitrons, which were rated at 20 kv and 100,000 amps peak current, replaced the spark gap switch used in the original experiments by Reichenbach. They are gas

tubes which use an igniter submerged in a mercury pool to triger an arc discharge. Breakdown (switching time) is extremely rapid. The ringing period for the discharge circuit was six microseconds.

The ignitrons and capacitor were located directly beneath the accelerator as shown in Fig. 6 to keep circuit inductance low. The capacitor outer case was connected through brass bars to a heavy aluminum plate which supported the gun barrel. This entire unit was grounded as shown in Fig. 2, while the ignitron bases floated electrically at the potential of the capacitor. A phenolic bar with a grounded hook was attached to the ignitron base plate as a safety measure when working near the capacitor.

b. Ignitron firing circuits. The ignitrons required an extremely fast high voltage (1500-3000v) pulse to initiate breakdown. The pulser circuit shown in Fig. 7 utilized a 6268 thyratron which provided a 3000 volt pulse with a rise time of about .5 microseconds. The pulser circuit was isolated from the capacitor high voltage by pulse transformers. The four pulse transformers were air core units with 1:2 windings. All four primary windings were connected in parallel to the pulser unit, while the secondaries floated at capacitor potential.

The pulser thyratron was fired in turn by the external trigger circuit shown in Fig. 8 which provided a 180 volt trigger signal to the pulser. The trigger control panel is shown in Fig. 9. The pulser and pulser power supply are shown in Fig. 10.

c. High voltage units. The capacitor was charged with a 40 kv power

supply originally designed for spark photography work. This was modified to incorporate all high voltage controls for the system as shown in Figs. 11 and 12. A normally closed Jennings high voltage relay was connected in parallel with the power supply main switch. Opening of this switch shut down the power supply and also grounded the capacitor through a one megohm high voltage resistor. This resistor served as a power dissipator in the event the capacitor could not be discharged and the shot had to be aborted. It also bled residual capacitor energy to ground after a firing.

Charging was through a solenoid operated knife switch and a three megohm high voltage resistor. The charging (top) and abort (bottom) resistors and Jennings relay are shown in Fig. 13. A microammeter in series with a 600 megohm resistor was connected across the capacitor, giving a direct reading of capacitor potential.

Vacuum System

The plasma gun discharged into a fourteen-inch diameter bell jar. Since foil replacement between discharges required disassembly of the gun, two separate vacuum systems were used for rapid evacuation of the jar. Connections to the vacuum equipment were made through a heavy aluminum manifold which supported the jar as shown in detail in Fig. 4. Flange fittings with o-ring seals were used throughout the system. A large volume pump was used initially to "rough" the system down to a pressure of about five microns of mercury. This pump was then shut down and the high vacuum system was opened.

The roughing system (Fig. 13) consisted of a Welch 1397B pump and a two-inch Stokes gate valve. The high vacuum system (Fig. 14) used a Welch 1402B fore pump and a four-inch Veeco combination diffusion pump, baffle and liquid nitrogen cold trap. The diffusion pump and baffle were water cooled, with a flow switch (Fig. 9) incorporated in the water line. LN_2 level was maintained with a Johns and Frame automatic level control from a 50 liter nitrogen pressurized Dewar flask as shown in Fig. 15.

The vacuum control circuit shown in Fig. 16 was designed to protect the diffusion pump and to place all vacuum power controls in one convenient location. This circuit prevented power from reaching the diffusion pump heating element if either the coolant water flow or the fore pump power was interrupted. The diffusion pump required a manual reset in either event, thereby preventing burnout or operation at excessive pressure (above 525 microns). Vacuum system controls are shown in Fig. 10.

A vacuum level of 5×10^{-6} millimeters of mercury or better was attainable. Even lower vacuums could be attained if required for future tests by replacing the lucite insulator shown in Fig. 3 with a material less subject to outgassing.

Instrumentation

a. Image converter camera. The high speed plasma front was photographed with the Abtronics Model 1 camera shown in Fig. 17. This camera uses an image converter tube as an electronically operated shutter capable of exposure times of .1, .3, 1, 3 and 6 microseconds. The four shutter tubes

have separate circuits which allow them to be triggered independently at any desired delay. Each channel has calibrated time delays up to 1000 microseconds.

The use of four separate objective lenses allows for individual adjustment of "f" stop or aperture so that each frame may be adjusted for the proper exposure density. Four Leitz f/1.5-50 mm objective lenses were used for this work.

A single loop of wire around one of the ignitron pulse transformers provided a 120 volt triggering pulse to the camera. When the four shutters were triggered at different delay times the movement of the plasma was recorded as four different images by the conventional Polariod camera which views the rear screen of all four shutter tubes. The average plasma velocity between images could then be determined from time-of-flight. Fig. 18 includes a photograph for a typical shot. Fig. 19 shows the camera location. Additional information on camera operation is presented in Appendix III.

b. Pressure measurement. A Veeco RG-31X combination thermocouple and ionization gage unit was used for pressure measuring. A gage of each type was connected to the bell jar manifold as shown in Fig. 4. The valve shown was closed to prevent overpressure on the ionization gage tube during firing. The high vacuum system was also equipped with separate vacuum gages. Pressure measuring controls are shown in Fig. 10.

c. Discharge monitoring. A radial loop of wire fastened to the undersurface of the capacitor upper plate was used to pick up an induced discharge

current pulse and give a dI/dt trace on an oscilloscope. A 10:1 probe in series with 20 megohms was used to attenuate the dI/dt signal to the oscilloscope.

The image converter camera was equipped with a monitor output which produced a signal for each of the voltage pulses which trigger the shutter tubes. This monitor output was also connected to the oscilloscope. A Techtronics type 551 dual-beam oscilloscope with camera attachment provided a photographic record of both dI/dt and the Abtronics monitor on a single Polaroid print (Fig. 18). The oscilloscope was set for a single sweep using the first pulse from the image converter camera monitor as a trigger.

4. Plasma Gun Experimental Firing Procedure.

A large number of tests were performed to develop discharge monitoring techniques, and then to prove that the firing of successive shots under uniform conditions would produce uniform diagnostic results. Some of this work is described in Appendices II and III. The firing of a typical shot will be described here.

In preparation for a firing, the bell jar, collector cylinder, and accelerator electrodes were removed and cleaned thoroughly with a solvent (acetone). Fine abrasive paper was used to polish portions of the electrodes which contacted the foil. The gun was then reassembled with a foil in place. A clean collector sheet was placed in the glass cylinder and the cylinder was slipped over the gun barrel.

The bell jar was then lowered and the valve was opened to the roughing

vacuum system. At a pressure of 5-10 microns a transfer was made to the high vacuum system. When the desired pressure was reached, the instrumentation was checked for proper operation, the capacitor was charged, and the discharge was triggered. Checklists which were used to insure that the detailed operations were performed in the proper sequence are given in Appendix I.

After a shot the collector sheet was removed and sprayed with lacquer to insure against accidental removal of the deposited material during handling. The collector sheet was then marked and circular sample disks .730 inches in diameter were removed using a sharp edged punch as shown in Fig. 20. Samples were normally taken at one inch intervals along the collector. The sample disks were then stored as shown in boxes until such time as the tracer analysis could be performed. The shot number was marked on the sample box and all data for that firing were recorded in the experiment log.[3] A number was assigned to each sample disk. For example, 17C-8 corresponds to accelerator shot 17. The letter denotes peripheral location on the collector sheet, i.e., left (L), right (R), or center (C) of the flattened sheet, and the last digits give the distance in inches to the sample center from the bottom of the collector sheet.

5. Tracer Analysis Theory.

In this experiment the mass of gold present on samples in trace amounts is determined by activation of the gold by neutron capture and observation of the radioactivity induced.

Since a neutron has no net charge, it cannot be detected like a charged particle. Instead, the neutron must somehow create an energetic charged particle which can be detected. One way this can occur is through induced radioactivity as in the reaction

$$n + Au^{197} \longrightarrow Au^{198*} \longrightarrow Au^{198} + \gamma$$

where the interaction of a neutron (n) with a gold atom produces a radioactive (*) residual nucleus which decays emitting gamma (γ) radiation.

Gamma-rays may be detected in many ways but a scintillation counter is the most versatile and is the most used counter in modern nuclear research. [11] Scintillation detection is a two-stage process. In such counters a material such as a sodium iodide crystal is used which converts the energy of the particle to be measured into photons at or near the wave length of visible light. A photomultiplier tube then converts the light flashes into electric pulses. [20] This tube is a device in which photons strike a cathode and emit secondary electrons which in turn strike a second electrode emitting still more secondaries, etc. The resulting multiplying effect for 9 or 10 stages is 10^5 or 10^6 and the short resolving times possible permit high counting rates.

The output of a scintillation counter is proportional to the initial number of photons so that the device has energy selective properties. When used in conjunction with pulse height analysing equipment which sorts the output pulses according to their energy, a distribution such as that in Fig. 21 (for gold 198) is obtained. The large peak, called the "photopeak", is produced

by the photoelectric process within the scintillation counter. The other peaks are produced by other scattering and shielding effects. Ref. 13 gives the characteristic gamma-ray spectrums for most materials and describes these effects more fully.

Since each material has its own characteristic spectrum, a pulse height analysis can be used for identification of unknowns. For quantitative information the amount of a material present is proportional to the total number of counts so that the area under the photopeak can be used in determining the mass. This depends, of course, on the initial level of radioactivity and the age of the sample. If a count is available for a known mass of a material, and providing the radiation dose and time since irradiation are the same for both the known and unknown masses, the unknown mass can be determined from

$$\text{(1)} \qquad \text{unknown mass} = \frac{\text{activity of unknown}}{\text{activity of control}} \text{ (control mass)} \quad .$$

This assumes that the period of observation of both is long enough to give a reliable count, realizing the random statistical nature of radioactive disintegrations.

A pulse height analysis is used to identify materials and to determine such things as the energy band of interest, the type of detection equipment required, background effects, and the activity necessary for accurate counting. Once this information is obtained the relative activity (and therefore the mass) of a material can be obtained by simply totaling the counts produced within the energy band of interest by a scintillation counter.

6. Tracer Analysis Equipment.

Sample irradiation was performed in an Aerojet-General Nucleonics Model 201 reactor located in Building 224 at the U. S. Naval Postgraduate School. This reactor used uranium 235 enriched UO_2 fuel and polyethylene moderator and was licensed for operation up to 1000 watts. Sample disks were placed between polyethylene plugs in a long tubular phenolic rod which was inserted into the reactor a distance of 94.63 inches. The thermal neutron flux at this location in the reactor was known to be 4.5×10^7 neutrons/cm^2-watt-sec.

A schematic of the detection and analysing apparatus is given in Fig. 22. A small lucite sample holder which fit into the top of the scintillation counter was used to insure that the same geometry was presented to the detector for all sample disks. The detector was shielded in a 26 x 26 x 33 inch enclosure of lead bricks.

The Nuclear Data ND 180 units convert pulses from the scintillation counter into digital form and store this information in a 512 channel memory. Each channel corresponds to either the total number of counts received in a preselected time interval or to the total number of counts received in a narrow energy band. In the latter (pulse height analyser) mode the equipment is preset for a total time of observation of from one to 30 minutes "live time" and automatically compensates for counting losses ("dead time") due to closely spaced pulses.

Controls on the ND 180M unit permit varying the width of the energy "window", or band, corresponding to each channel, and adjustment of the

threshold above which pulses are accepted. Appropriate settings for the gold analysis were determined using spectrums of known elements and these settings were not changed during the experiment. The M-unit settings used were as follows:

Coarse Gain	2
Fine Gain	10.0
Zero Level	9.34/COARSE
Threshold	0
Coincidence	FREE

At the end of an observation the decay curve or energy spectrum (depending on the mode used) stored in the memory can be either displayed on the oscilloscope or printed out in digital form on the teletype machine.

7. Tracer Analysis Procedure.

Two methods of performing the experiment were considered. In the first the gold foil would be irradiated, placed in the accelerator and fired. After firing, sample disks would be cut from the collector sheet and the amount of gold present determined using appropriate radiation detection devices. This system, though satisfactory, introduces several difficulties which will be discussed.

The experiment was actually performed by first firing the shot, then irradiating the sample disks and monitoring their characteristic gold radiation. This method had several advantages:

a. Radioactive materials did not leave the Reactor Facility.

b. The plasma gun, vacuum system and surrounding area were not contaminated, therefore monitoring and frequent disassembly for cleaning were avoided.

c. The total amount of radioactive material handled was quite small, since only about one third of the gold was vaporized, only a very small portion was deposited, and only a portion of that gold deposited was sampled.

d. The tracer analysis could be performed at any time after the firing, eliminating the rush to get all samples counted before they decayed appreciably. The samples could also be sent away for analysis by another radiation laboratory at a later date.

The principal disadvantage of the procedure used was that the collector material becomes activated along with the gold and produces a background count which could interfere with the gold count. The use of pure aluminum for the collector sheet eliminated this problem. The small activation cross section and short half-life of aluminum produced effects which were negligible if the samples were allowed to decay for two or more hours before counting. A study of plasma deposition on walls of other materials could require the use of the first experimental procedure considered.

Approval for use of the Postgraduate School Reactor Facility was obtained after submission of written requests [4] describing the experiment and completion of Atomic Energy Commission Form 313. All handling of radioisotopes was in accordance with the safety rules given in Ref. 14.

A rough estimate of the amount of deposited gold to expect on a typical sample disk was made utilizing Ref. 19. From this estimate it was determined that a radiation dose of 100 watts reactor power for 10 minutes would produce activity sufficient for gold detection. Trial runs demonstrated this to be true and this standard dose was used for all subsequent tracer work.

A control sample disk with a known weight of gold was prepared as described in Appendix IV and irradiated. After removal from the reactor and allowance of a few hours for aluminum decay, the control was placed in the scintillation counter and the Nuclear Data units were used in the pulse height analyser (PHA) mode to obtain an energy spectrum as in Fig. 21. This counting was repeated several times during the next two or three days as the gold decayed. The counting time was increased as the gold decayed to insure sufficient counts for a smooth curve.

Since the amount of gold present at any time is proportional to the area under the 411 kev photopeak, only this peak (20 channels either side of the channel with maximum count) was plotted from the PHA output data as shown in the example of Fig. 23. Area under the peak was then measured with a planimeter. Since counts were made for different counting times, and curves were plotted to different scales, the activity was computed using

$$A = SVH/60t$$

where

A is sample activity in counts/second

S is area under the photopeak in square inches

V is the vertical scale in counts/inch

H is the horizontal scale in channels/inch

t is the length of the counting period in minutes

A curve giving activity as a function of time-since-irradiation was then plotted (Fig. 24) for the control sample. This curve was then used to obtain a control activity at any time for use in equation (1). As a check on the validity of equation (1) for trace amounts of unknown, a sample taken at random from one firing was irradiated with the standard dose and monitored as shown in Fig. 24 as it decayed.

A tracer analysis was also run on a blank aluminum disk as a check on background count due to aluminum activity. It was found that the one-mil foil finally used produced little radiation after about two hours and that a value of 20 counts per channel could be used across the energy band of interest as background for a ten-minute count time at 10-30 hours after irradiation. In computing sample activity only the area above this value was used.

For subsequent runs the unknowns were irradiated one day and placed in the detector apparatus the following day. Samples were irradiated in stacks of six at one time and a counting period of ten minutes per sample was normally used. The photopeak was plotted for each sample and the activity computed in the same manner as for the control. Data for all tracer work are found in Ref. 3. The activity for a known mass of gold of the same age (time since activation) as the unknown was obtained from a curve such

as Fig. 24.

8. Results and Discussion.

Accelerator System

A major portion of the time and effort spent on this project was involved with design, component procurement, and development of the accelerator system described in Section 3 of this report. Procedures were established for operation of the system and are given in checklist form in Appendix I.

Calibration of the capacitor and of the high speed camera are discussed in Appendices II and III respectively. As a check on both the accelerator system and the discharge monitoring equipment a series of six identical firings was made using the same capacitor voltage and the same vacuum system pressure. In this way the reproducibility of test results was noted. For these tests a capacitor voltage of 15.5 kv and a pressure of 5×10^{-4} mm. of mercury were used.

The results of this test series are given in Table I. The two film records (as in Fig. 18) for each shot were used to determine distance traveled by the plasma front versus time. On the image converter photographs the distance traveled was measured to the end of the visible light front using the spaced markings on the collector cylinder (Fig. 18A). The elapsed time between firing of the shutter tubes was obtained from the oscilloscope trace (Fig. 18B) of the Abtronics camera monitor. Accuracy of this distance determination appears to be about 1.0 cm.

The velocity of the plasma front was obtained by measuring the slope of

the distance versus time curves given in Figs. 25-30. A straight line was used to determine the average velocity during the time of observation. There does, however, appear to be a downward trend near the top of these curves indicating a slight decrease in velocity near the end of the 20 centimeters under observation. Average velocities obtained from this series of firings are given in Table II. For firing under these conditions the velocity measured for each shot was within 8% of the 3.60 cm/microsecond (118,000 ft/sec) mean velocity. This appears to be a good degree of reproducibility for the anticipated uses of the system.

A possible cause of differences in the measured velocity was thought to be slight variations in pressure from one run to the next. The ionization gage valve and main vacuum valve were closed before accelerator discharge to prevent gage exposure to excessive pressure and system contamination. Since this resulted in some pressure increase before discharge, an attempt was made to compensate by pumping to a slightly lower pressure than that desired before closing the valves.

To observe the effect of discharge pressure on velocity, another series of tests was performed using the same capacitor charge and discharging to different pressures. It was found that improving the vacuum by $1\frac{1}{2}$ orders of magnitude to 1×10^{-5} mm Hg gave a 3.9 cm/microsecond velocity. Velocity of the exhaust plasma is therefore not sensitive to small pressure change at the low pressures being considered, and differences in measured velocity are more likely to be due to the accuracy of measurement than to slight pres-

sure uncertainty. The maximum attainable velocity for exhausting into a perfect vacuum appears to be about four cm/microsecond for this plasma gun system with a 15.5 kv maximum capacitor charge.

Tracer Analysis

Several firings and a considerable number of tracer runs were made in attempts to find a suitable collector material. It was found that impurities (such as magnesium) common in most aluminum sheet produced sufficient radiation to mask the trace gold deposits. Even commercially prepared high purity aluminum was found to be unacceptable for this reason. It was surprising, therefore, to find that ordinary household aluminum foil was far superior and produced negligible background interference. Since this foil was only one mil thick in the heavy duty grade, small spring clips were required to hold collector sheets in place. No interference problems were experienced after changing to this material.

Monitoring the decay of a control sample disk with a known mass of gold along with an unknown sample given the same radiation dose (Fig. 24) showed that the ratio of activities of the two stayed nearly constant over a two-day period as evidenced by the parallel decay curves on a semi-logarithmic plot. The curve of Fig. 31 was obtained using the final tracer apparatus configuration and a control disk with 1264 micrograms of gold. Values from this curve were used in equation (1).

Portions of two accelerator runs, 17 and 19, were analysed. These two shots were fired under identical conditions (15.5 kv and 1×10^{-5} mm Hg)

using the final collector configuration: one-mil aluminum foil. These results are presented in Tables III and IV and Fig. 32. Fig. 32 indicates a considerable difference (a factor of three) in deposition rate from one side to the other on the collector sheet for shot 19. Possible reasons for the large difference are:

(a) Actual mass deposited from the plasma is not axially symmetric and/or is not the same for succeeding firings. This is unlikely for reasons outlined in (c) below but must be determined from further tests. Foil wrinkles or an unsymmetrical electrical path caused by uneven clamping pressure on the foil could possibly cause such nonuniformities.

(b) Samples did not all receive the same radiation dose. This seems unlikely since the 19L samples were irradiated in two separate batches; one for the even numbered samples, 2-4-6-8-10-12, and one for the odd, with a fairly continuous curve resulting. It is possible, however, that a day-to-day variation in dosage was the cause, since 19L and 19R samples were irradiated on different days and such factors as reactor core temperature or slight variations in insertion distance into the core could affect the neutron flux. This possibility should be easily resolved by inclusion of a control sample in each group of samples irradiated.

(c) Drift or malfunction of detection equipment from day to day. The first possibility was largely eliminated earlier by observation of samples over longer periods and obtaining smooth decay curves as in Fig. 24. It is most probable that the detection apparatus was not operating properly for the an-

alysis of 19L samples, since Fig. 32 indicates that the total amount of deposited gold for these samples was about nine milligrams or over 50% of the mass vaporized. Losses this large would probably be accompanied by a pronounced decrease in plasma luminosity which did not occur. Transient problems which were experienced with the new detection equipment were probably responsible. Once again, inclusion of a control disk as a monitor as suggested in (b) would eliminate this possibility and is recommended for future tracer runs.

Although insufficient tests were performed to make an exact determination of total gold deposition, the results of Fig. 32 give a rough estimate for the case of a 15.5 kv discharge to a 10^{-5} mm vacuum. Assuming a distribution around the cylindrical collector as indicated by the samples of curve 19R gives a total of 2.9 milligrams of gold deposited in a 12-inch distance above the gun muzzle. This is approximately 19% of the mass initially vaporized and is an indication of the significant amount of mass loss possible from a metalized plasma flow to surrounding walls. Follow-on tests to determine deposition as a function of various flow parameters and to measure deposition inside the accelerator electrodes are presently planned.

For each of the tracer runs described in this report the gold photopeak was actually plotted and its area measured. From these curves the background effects could be evaluated and parameters such as required radiation dosage, detection equipment settings, required count time, and desired age at the time of counting were determined. For future tests this tedious pro-

cedure can be eliminated and the sample activity determined simply by addition of the total counts in the energy band of interest. If the procedures and equipment settings recommended herein are used, sample activity can be obtained by addition of counts for the 41 channels bracketing the channel recording the maximum count.

The tracer studies performed to date have demonstrated that sufficient gold was deposited to be easily and accurately detected using the equipment and methods described. One change in procedures is recommended, i.e., that a control disk be included as a monitor with each group of samples irradiated until sufficient data are accumulated to prove this unnecessary.

9. Conclusions.

The coaxial plasma accelerator and associated systems function satisfactorily. Procedures were established which make safe and reliable operation of the equipment possible. The system produced plasma slugs with measured velocities up to 3.9 centimeters per microsecond which were reproducible within about 10% using an image converter camera for velocity determination. The vacuum system can provide a vacuum of the order of 10^{-6} mm. of mercury.

A technique was developed for radioisotope tracing of gold deposited on a collector near the plasma gun exhaust. Preliminary tests for one set of discharge conditions indicate that approximately 20% of the gold plasma initially formed is deposited inside a 2.4 inch diameter aluminum cylinder surrounding the first 12 inches of flow.

10. Suggestions for Further Investigation.

The plasma gun described in this report is a flexible device which suggests a large number of possible experiments. Current ideas include:

(a) A parametric study of mass deposition with varying capacitor voltage and various collector cylinder diameters.

(b) Investigation of the depositing of material inside the gun barrel by designing electrodes from which samples can be taken.

(c) Study of various electrode configurations.

For future tests it is recommended that the following procedures be used:

(a) A control disk should be included as a monitor with each group of samples irradiated.

(b) It is recommended that the integrity of the foil electrical connection be checked by measuring and recording the resistance across the accelerator electrodes before each discharge.

(c) Consideration should be given to incorporation of a "crowbar" circuit into the discharge system. This would make it possible to abruptly terminate current flow to the electrodes at any desired time, producing a shorter, more well defined plasma slug.

BIBLIOGRAPHY

1. Ashby, D., Gooding, T.J., Hayworth, B.R., and Carson, A.V. Exhaust Measurements from a Pulsed Coaxial Gun. AIAA Journal, 1965, Vol. 3, No. 6, pp 1140-1142.

2. Bostick, W.H. Hall Currents and Vortices in the Coaxial Plasma Accelerator. Physics of Fluids, 1963, Vol. 6, No. 11.

3. Brumwell, R.K. Plasma Accelerator Experiment Record and Data Log USNPGS, 1966.

4. Brumwell, R.K. Request for Use of USNPGS Reactor Facilities. Letter to Radiological Safety and Isotopes Committee, USNPGS, and Reactor Operating Committee, USNPGS, 12 January 1966.

5. Corliss, W.R. Propulsion System for Space Flight. McGraw-Hill, 1960.

6. Eubank, H.P. and Wilkerson, T.D. Ion Energy Analyser for Plasma Measurements. Review of Scientific Instruments, 1963, Vol. 34, No. 1, pp 12-18.

7. Ferraro, V.C. and Plumpton, C. Magneto-Fluid Mechanics. Oxford University Press, 1961.

8. Grossman, W. Experiments With a Coaxial Hall Current Plasma Accelerator. NASA Langley, 1964.

9. Guman, W.J. Switch Triggered Pulsed Plasma Accelerator Thrust Measurements. Republic Aviation, 1965.

10. Gooding, T.J. Development of a Coaxial Plasma Gun for Space Propulsion. General Dynamics/Astronautics, 1964.

11. Halliday, D. Introductory Nuclear Physics. Wiley, 1955.

12. Hart, P.J. Plasma Acceleration With Coaxial Electrodes. Lockhead Aircraft Corp., 1961.

13. Heath, R.L. Scintillation Spectrometry Gamma-Ray Spectrum Catalogue. Phillips Petroleum Co., 1957.

14. Jones, H.A. Radiological Safety and Isotopes Committee-Minutes. USNPGS, 20 December 1962.

15. Kash, S.W. Plasma Acceleration. Stanford University Press, 1960.

16. Keck, J.C., Fishman, F., and Petschek, H. Current Distribution and Flow Model for Large Radius MAST. Physics of Fluids, 1962, Vol. 5, No. 630.

17. Mannal, C. and Mather, N.W. Engineering Aspects of Magnetohydynamics. Columbia University Press, 1962.

18. Mostov, P.M., Neuringer, J.L., and Rigney, D.S. Electromagnetic Acceleration of a Plasma Slug. Republic Aviation, 1961.

19. Reichenbach, R.E. Personal Notes - Deposition of Metallic Plasmas on Cold Walls, 1962.

20. Valente, F.A. A Manual of Experiments in Reactor Physics, Macmillan, 1963.

21. Vlases, G.C. Phd Thesis. California Institute of Technology, 1963.

22. Zeimer, R.W. An Electromagetic Shock Tube for Aerodynamic Research. Space Technology Labs., 1958.

TABLE I

PLASMA VELOCITY MEASUREMENTS

15.5 KV Capacitor Voltage 5×10^{-4} mm Vacuum

	Frame 1		Frame 2		Frame 3		Frame 4	
Shot No.	t	d	t	d	t	d	t	d
11	8.8	7.6	10.2	10.2	11.4	17.0	12.9	20.3
12	8.9	7.6	10.1	8.9	11.4	17.0	12.9	20.3
13	8.3	3.3	9.7	7.6	11.1	14.0	12.4	16.0
14	8.3	6.1	9.5	8.6	11.0	16.0	12.5	17.8
16	8.3	4.1	9.5	8.9	10.7	15.2	12.0	16.8
18	8.3	3.8	9.4	7.6	10.8	15.2	11.7	16.5

t - Time after oscilloscope triggering, microseconds

d - Distance of plasma front from muzzle, centimeters

TABLE II

PLASMA VELOCITY

15.5 KV 5×10^{-4} mm Mecury

Shot No.	Measured Velocity - cm/ms
11	3.6
12	3.5
13	3.6
14	3.4
16	3.6
18	3.9

Mean Velocity 3.6 cm/ms

Maximum Deviation .3 cm/ms or 8.3%

TABLE III

TRACER RESULTS RUN 19L

Sample	Activated	Age hrs.	Activity counts/sec	Control Activity counts/sec	Mass μgms/in^2
1	1637 14 March 1637				
2		16.5	1.25	376	4.2
3		16.7	7.03	375	23.7
4		16.9	29.00	373	98.4
5		17.1	54.00	372	183.8
6		17.4	53.43	371	182.1
7	14 March 1648	19.2	49.27	362	172.2
8		19.4	45.83	361	160.4
9		19.6	37.60	361	131.7
10		19.9	28.35	360	99.6
11		20.1	28.30	359	99.6
12		21.5	11.91	352	42.8

TABLE IV

TRACER RESULTS RUNS 19R AND 17C

Run	Sample	Activated	Age hrs.	Activity counts/sec	Control Activity counts/sec	Mass $\mu gm/in^2$
19R	3	21 MARCH 1612	16.9	8.0	373	27.1
	5		17.1	2.93	372	9.96
	7		16.4	17.06	376	57.4
	9		16.2	15.00	377	50.3
	11		15.9	11.1	379	37.0
17C	5	10 MARCH 1056	22.6	11.2	346	40.9
	8		22.4	9.07	347	26.1

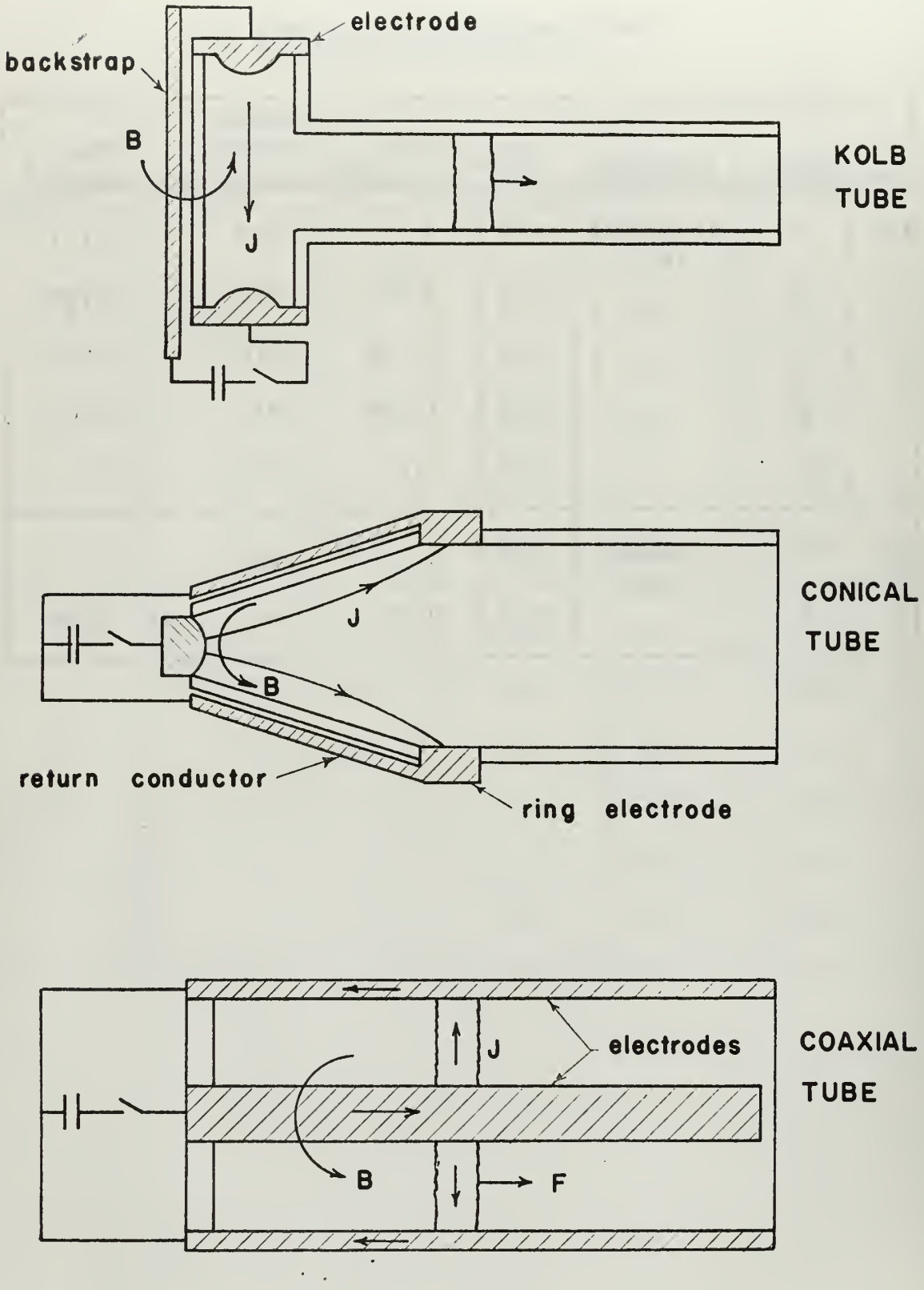


FIGURE 1
THREE ACCELERATORS

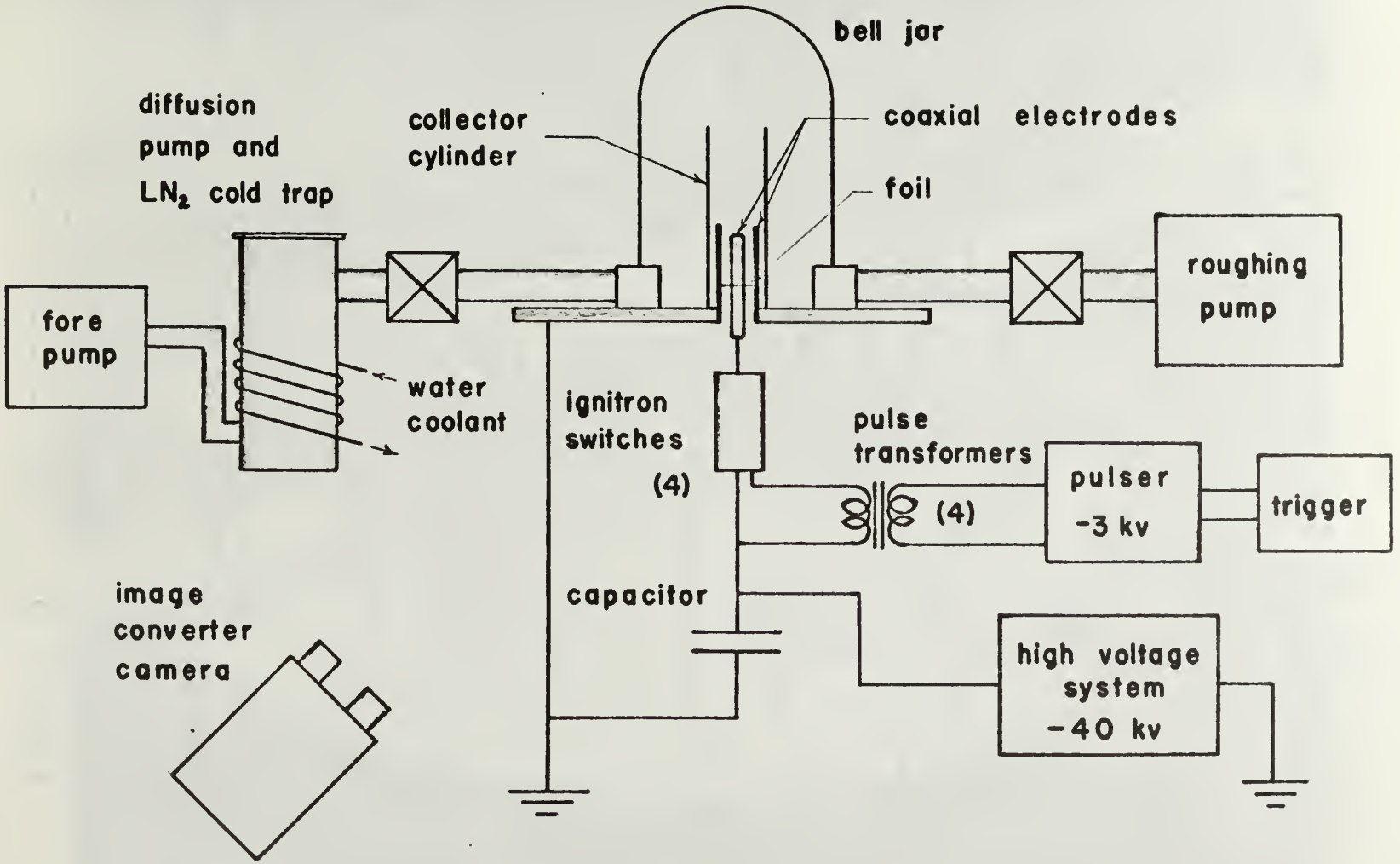


FIGURE 2 ACCELERATOR SYSTEM

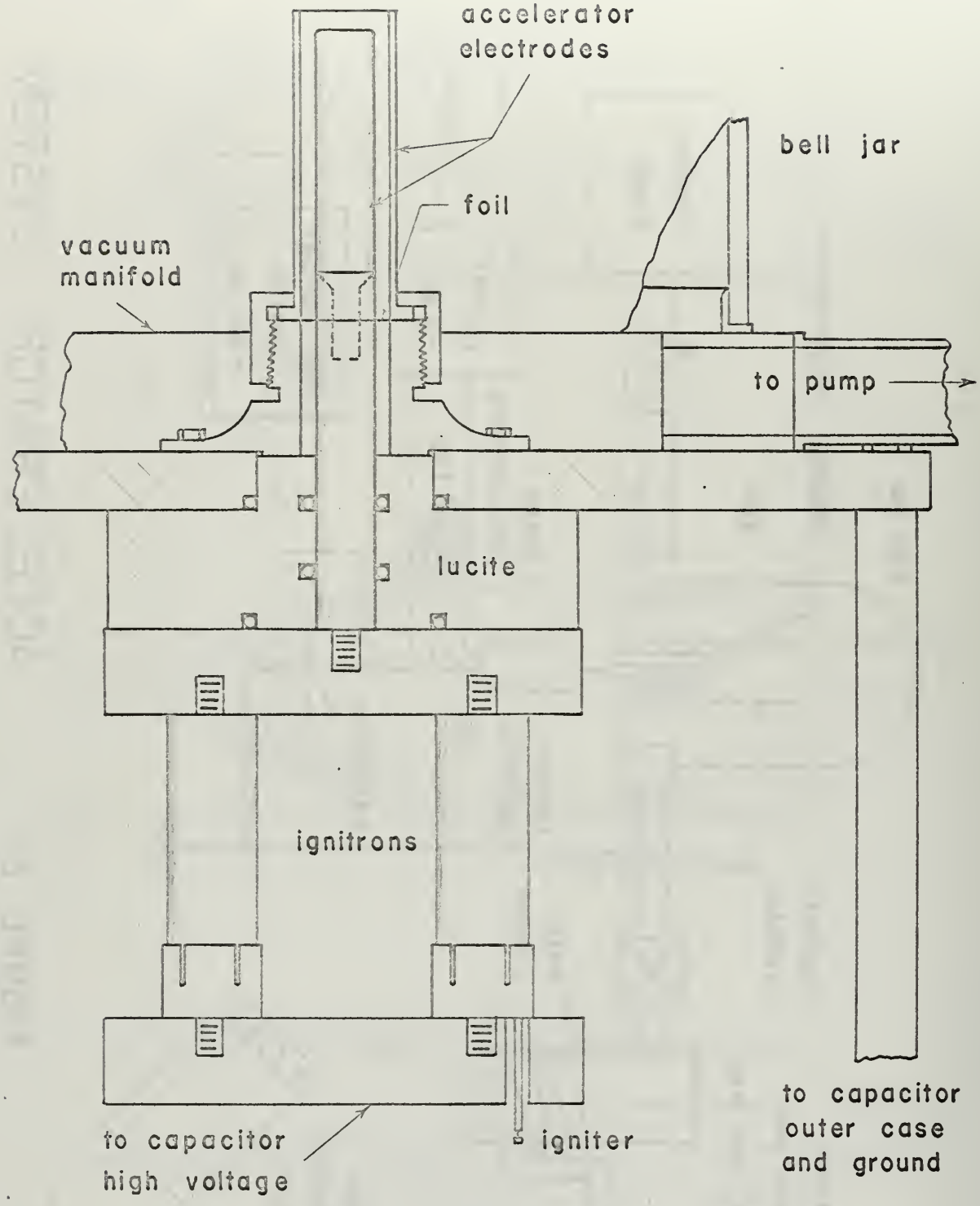


FIGURE 3 ACCELERATOR

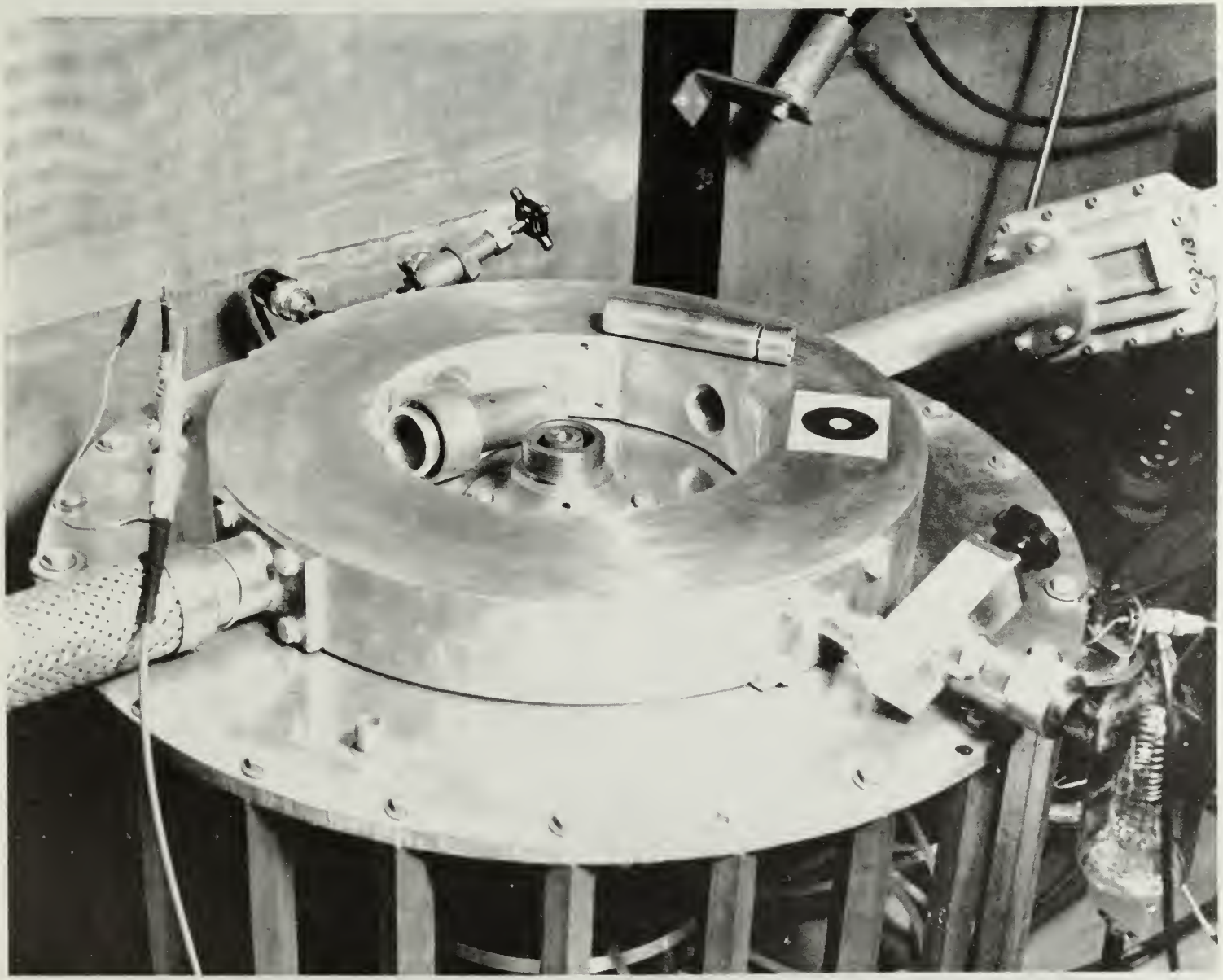


FIGURE 4 DISASSEMBLED GUN

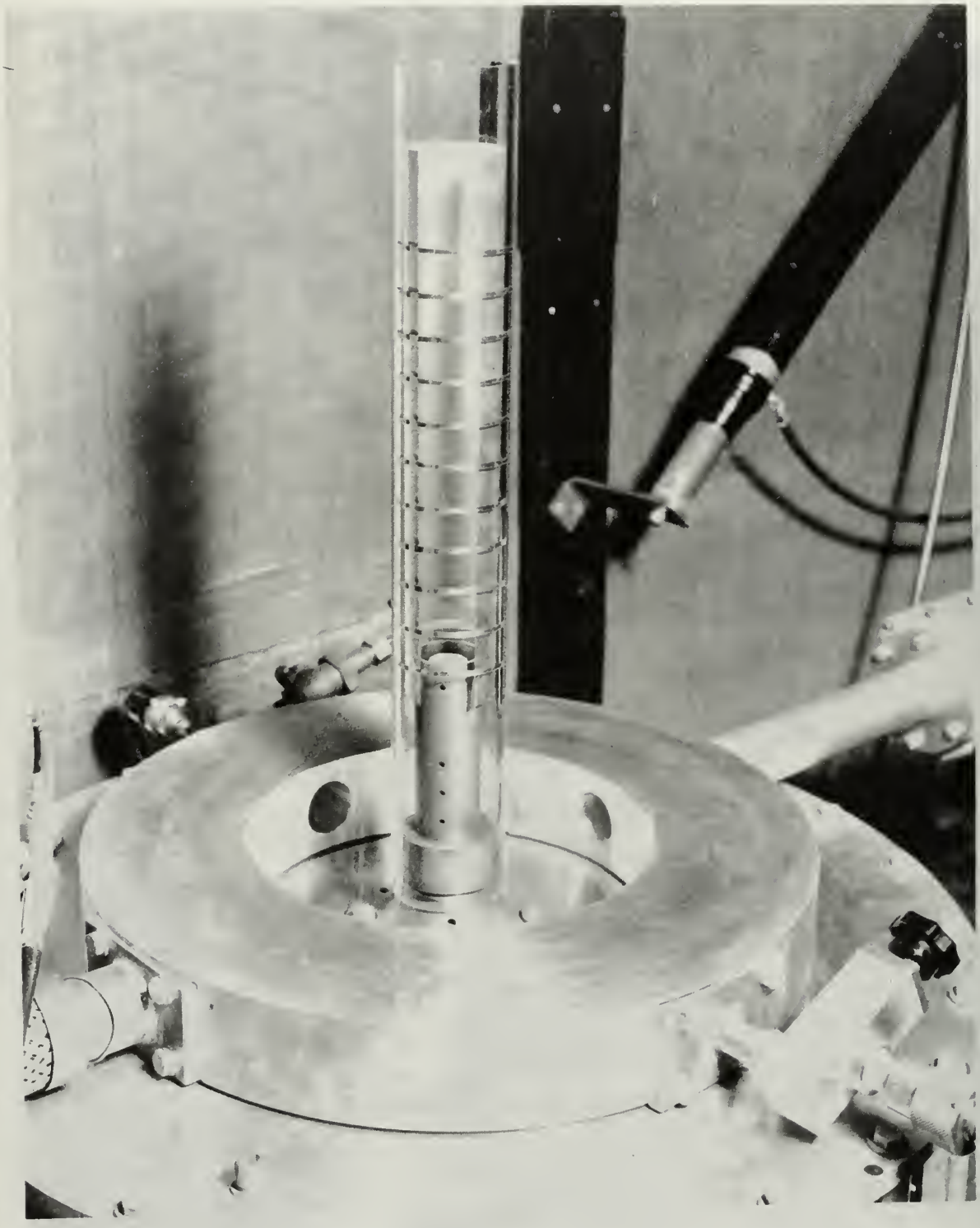


FIGURE 5

ASSEMBLED GUN

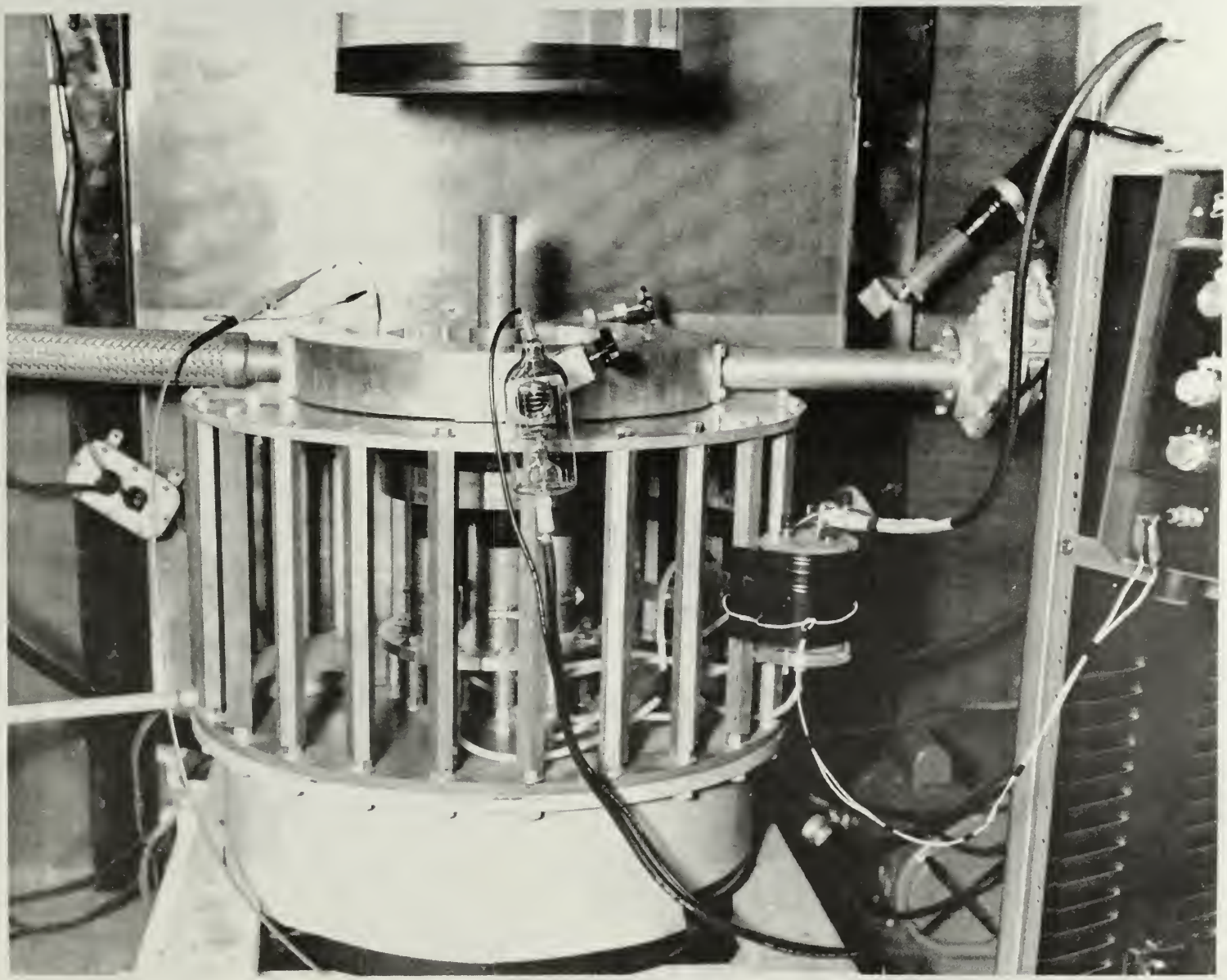


FIGURE 6 CAPACITOR and IGNITRONS

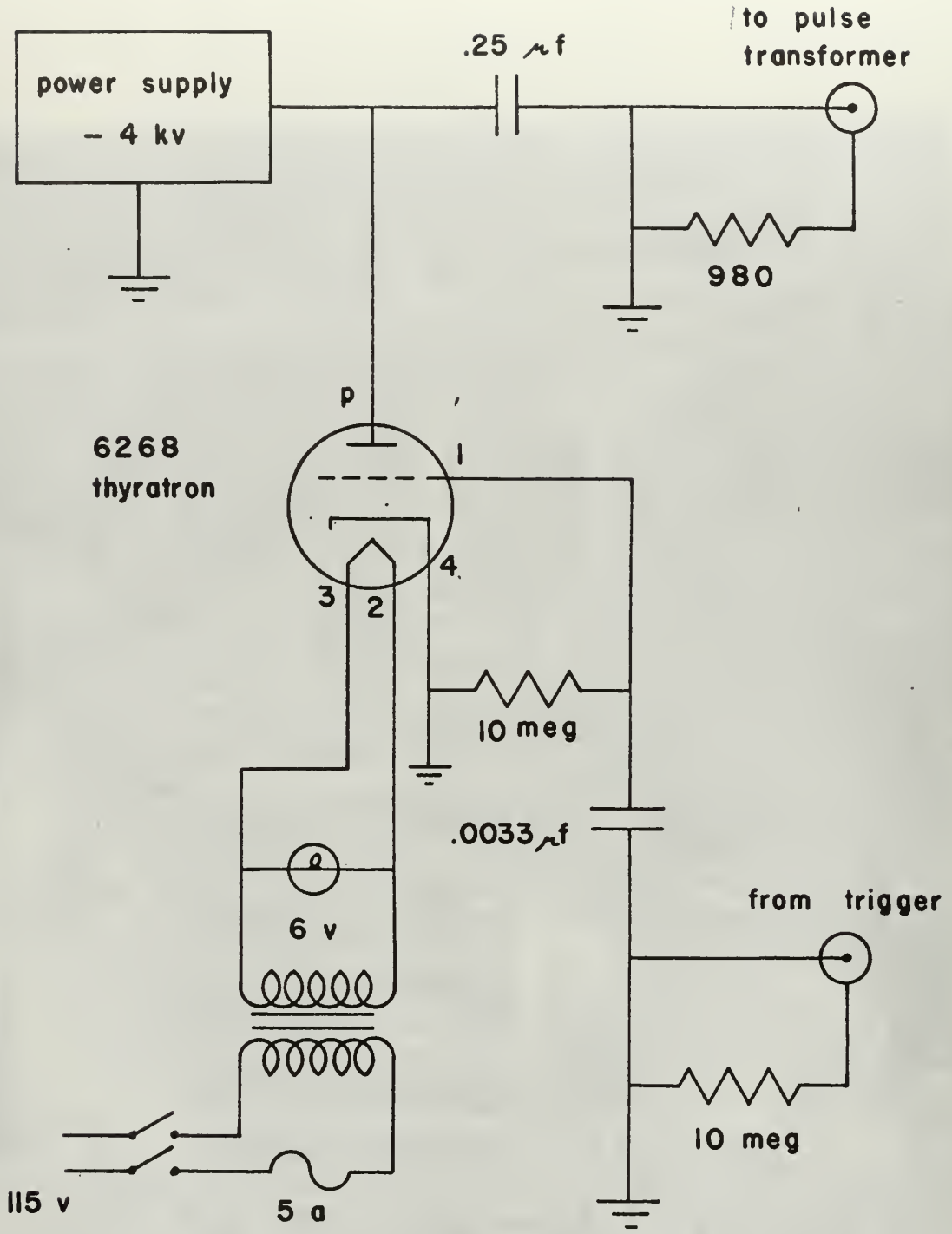


FIGURE 7. IGNITRON PULSER

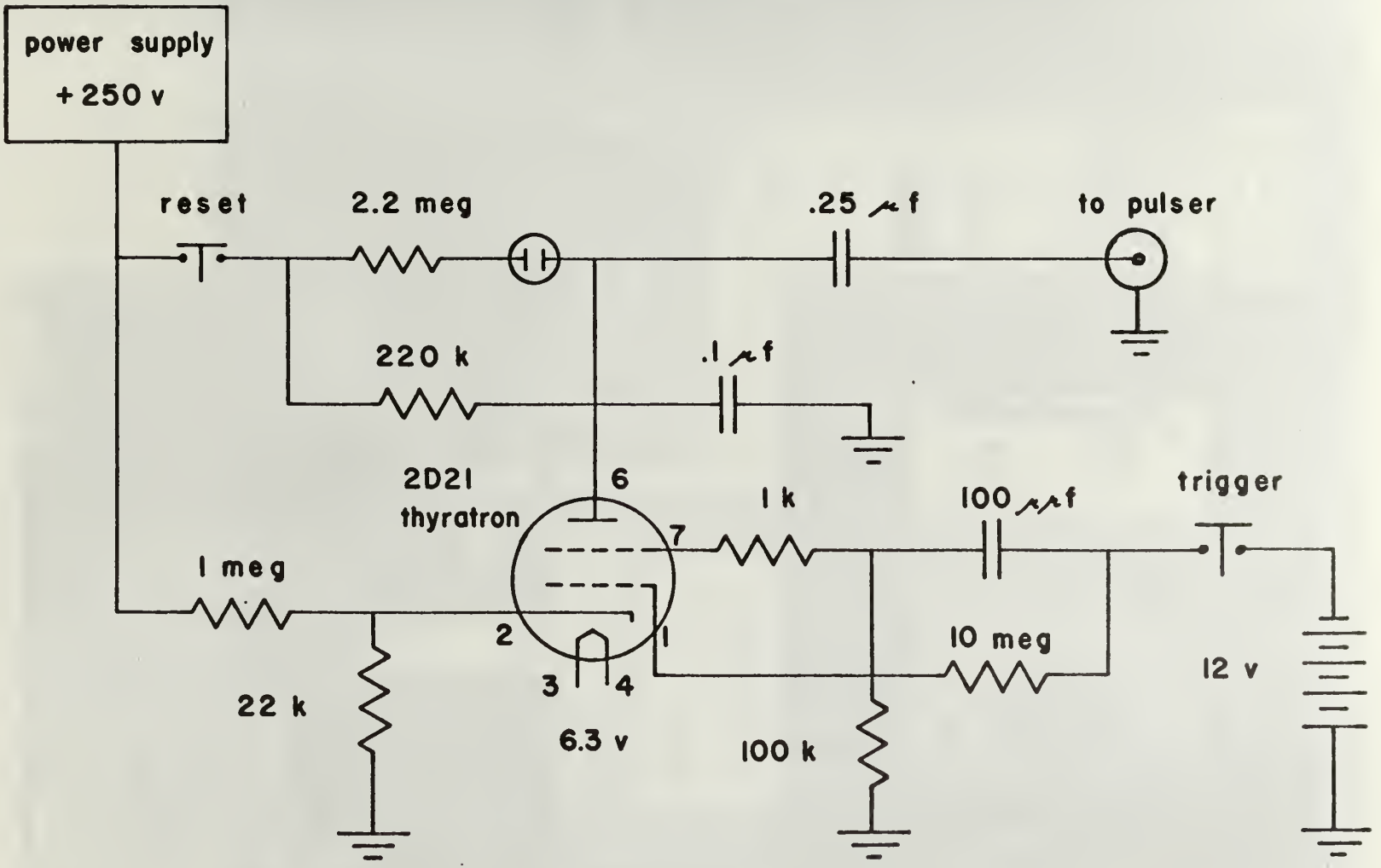


FIGURE 8 CAPACITOR DISCHARGE TRIGGER

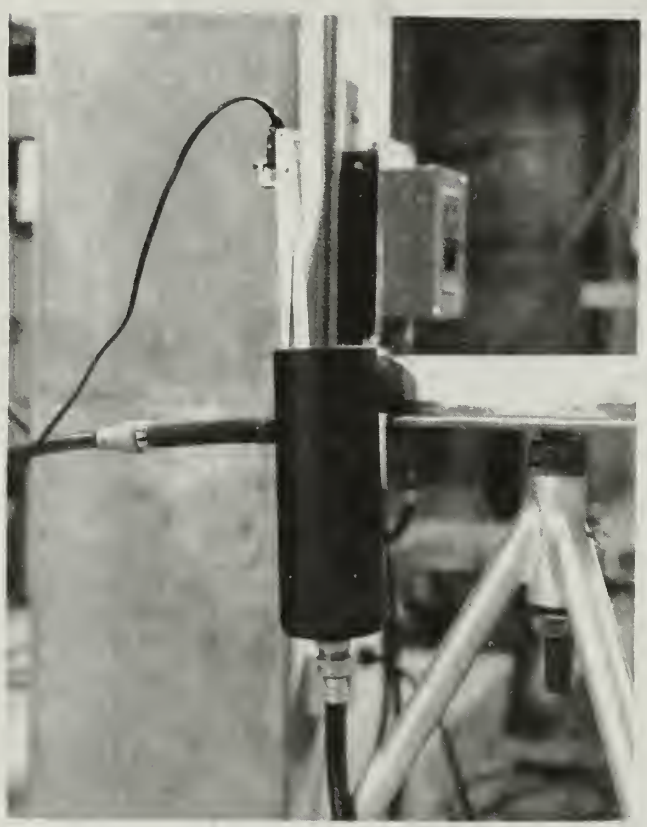


FIGURE 9A

FLOW SWITCH



FIGURE 9B

TRIGGER PANEL

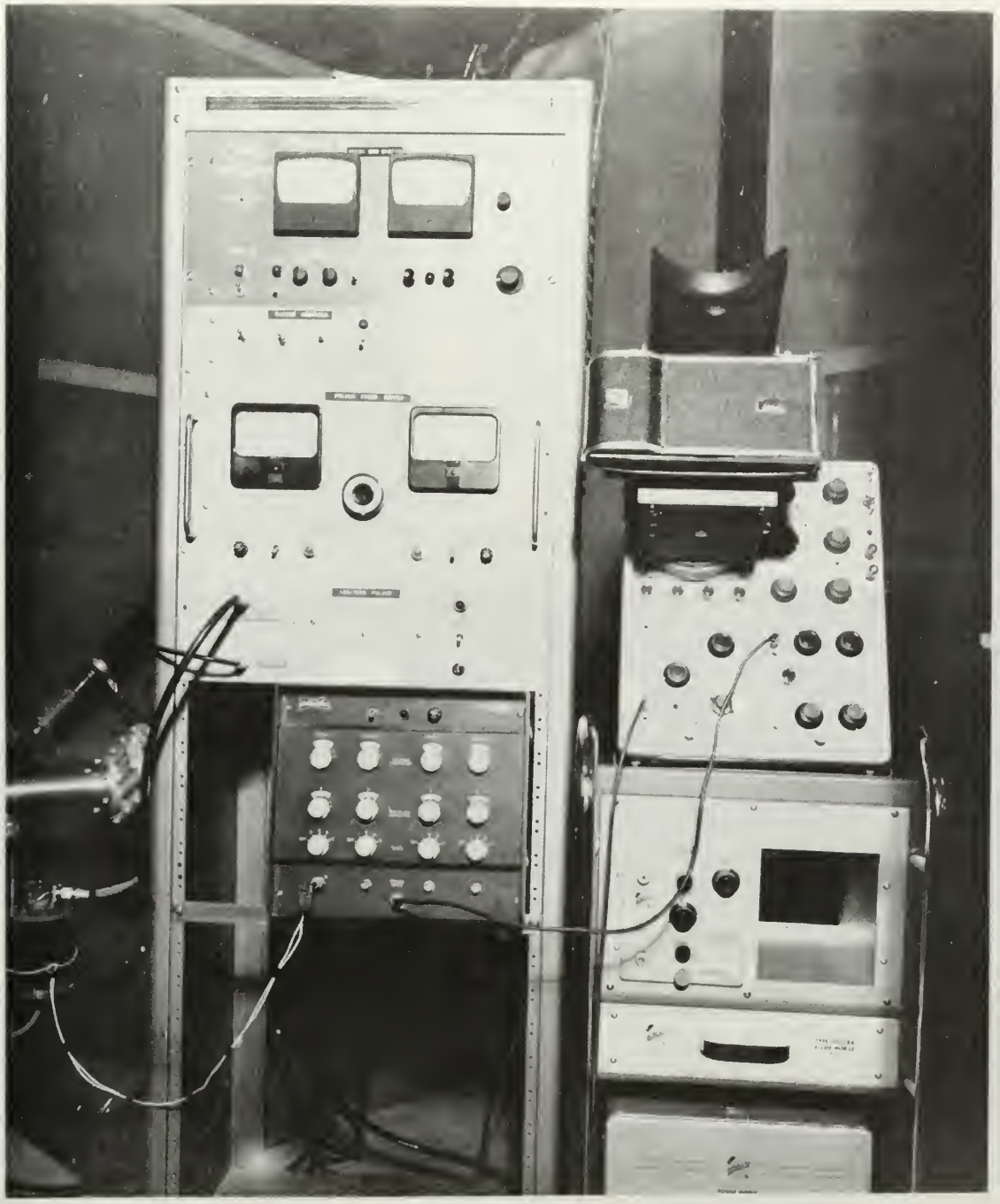


FIGURE 10

INSTRUMENTATION

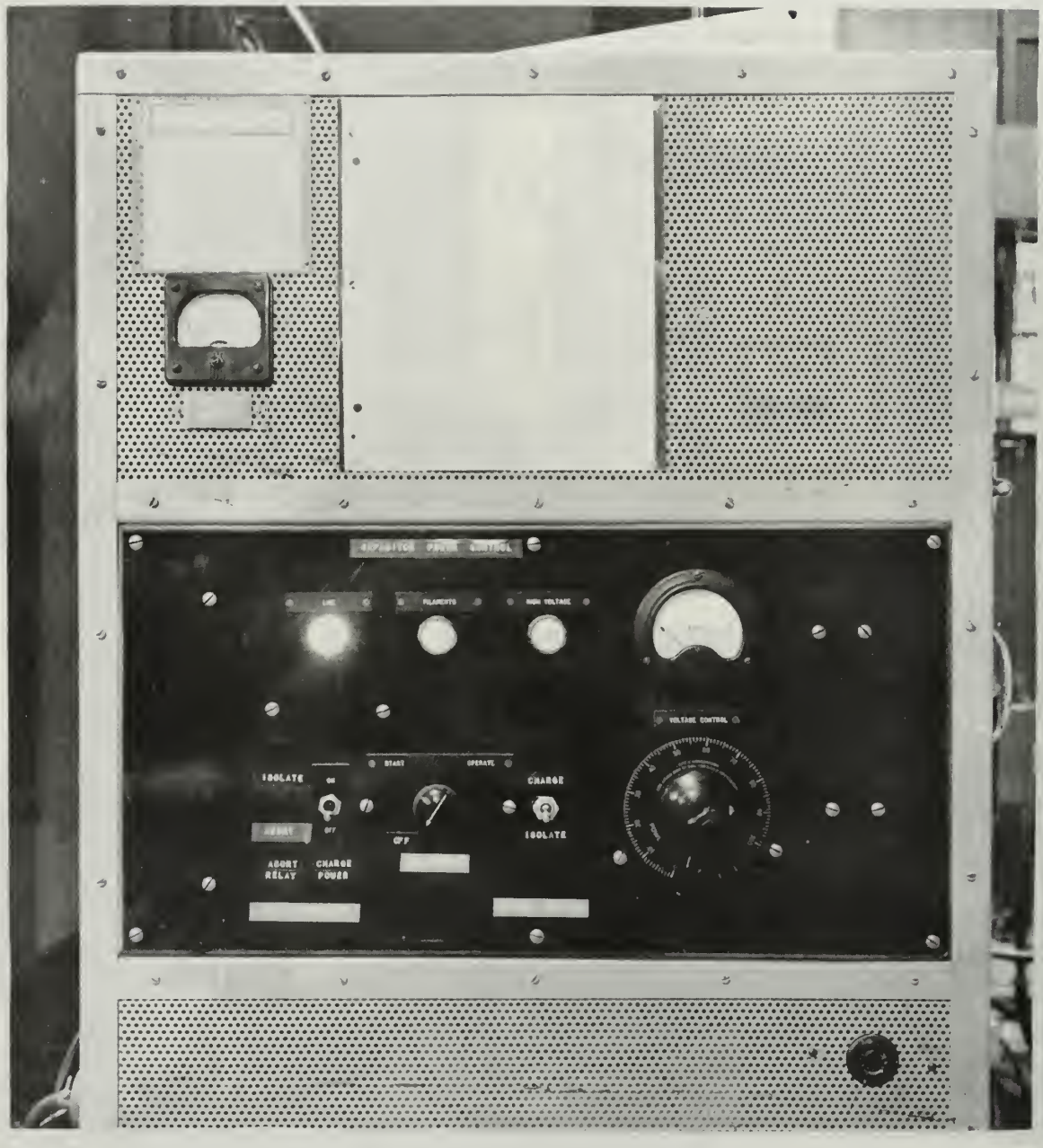


FIGURE 11

POWER CONTROL PANEL

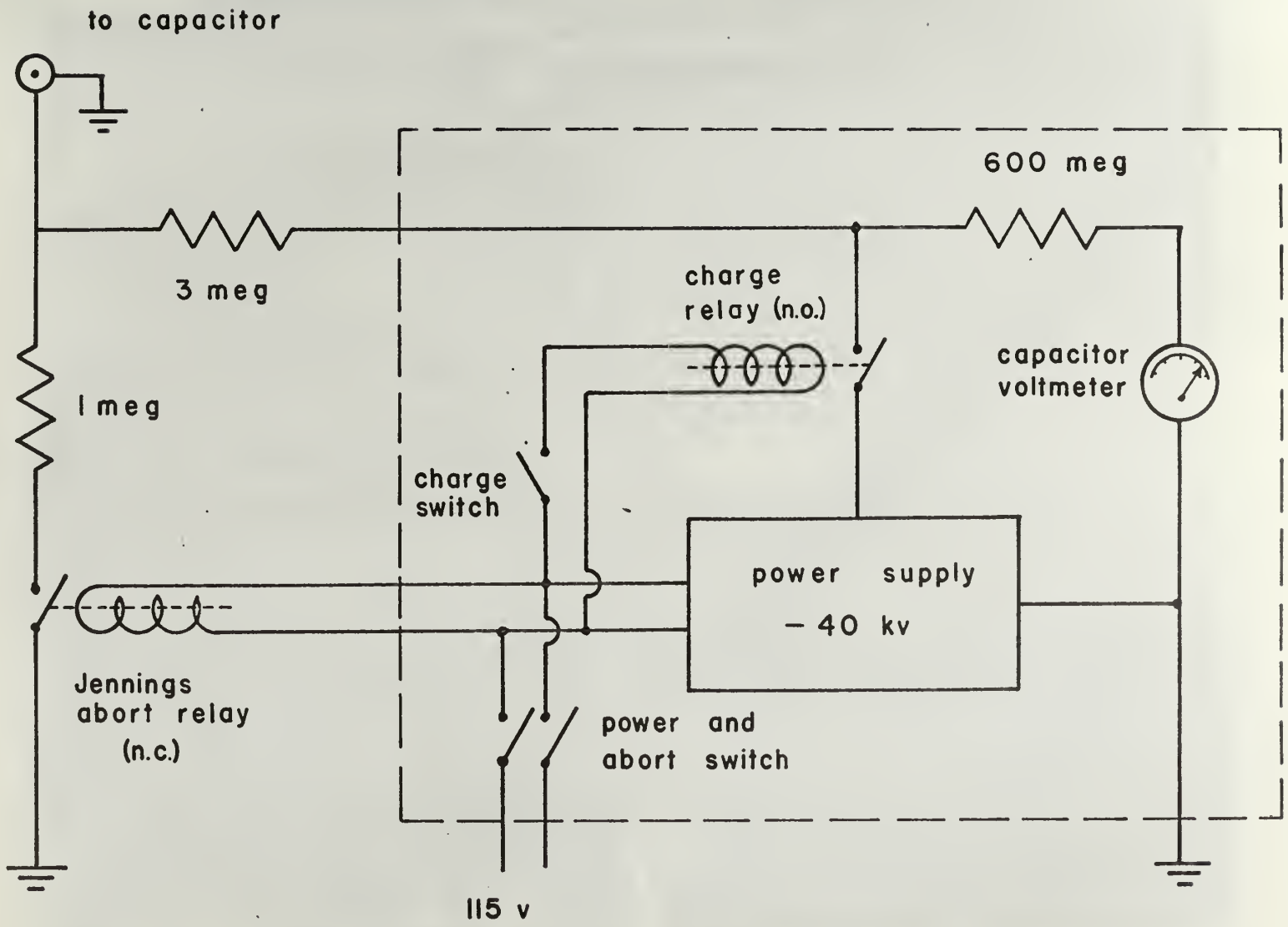


FIGURE 12 HIGH VOLTAGE SYSTEM

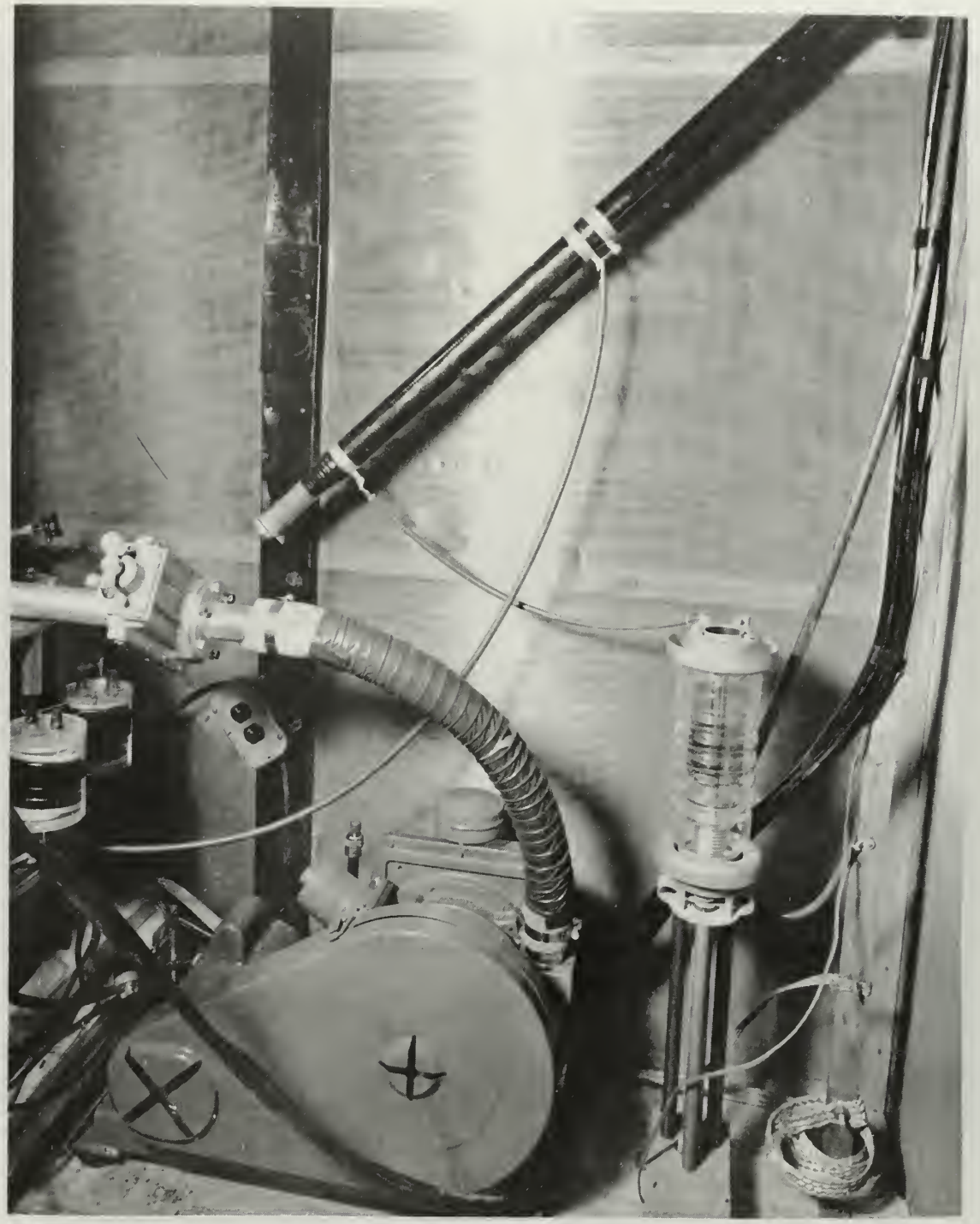


FIGURE 13

HIGH VOLUME VACUUM SYSTEM and
HIGH VOLTAGE COMPONENTS

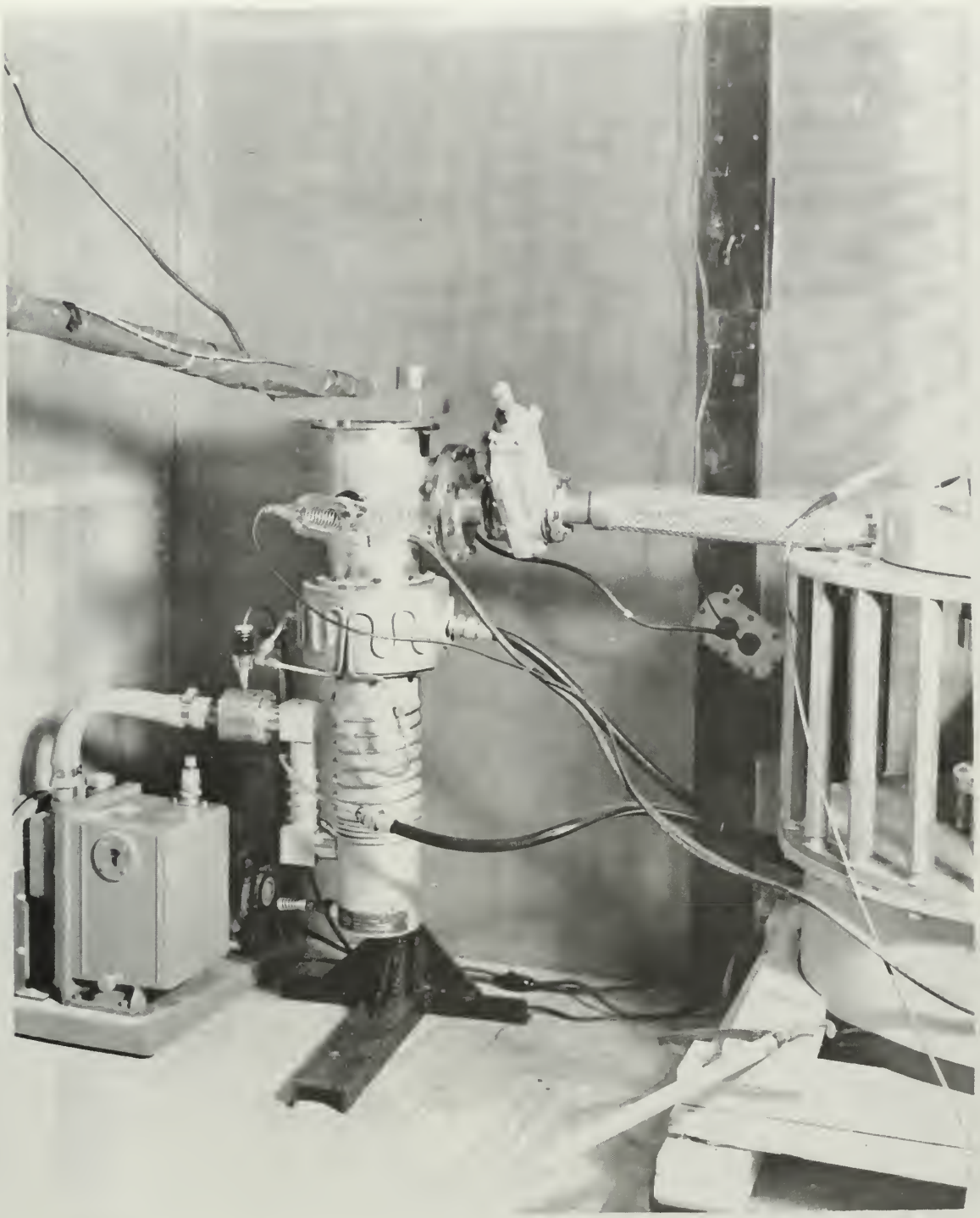


FIGURE 14

HIGH VACUUM SYSTEM



FIGURE 15

LIQUID NITROGEN SYSTEM

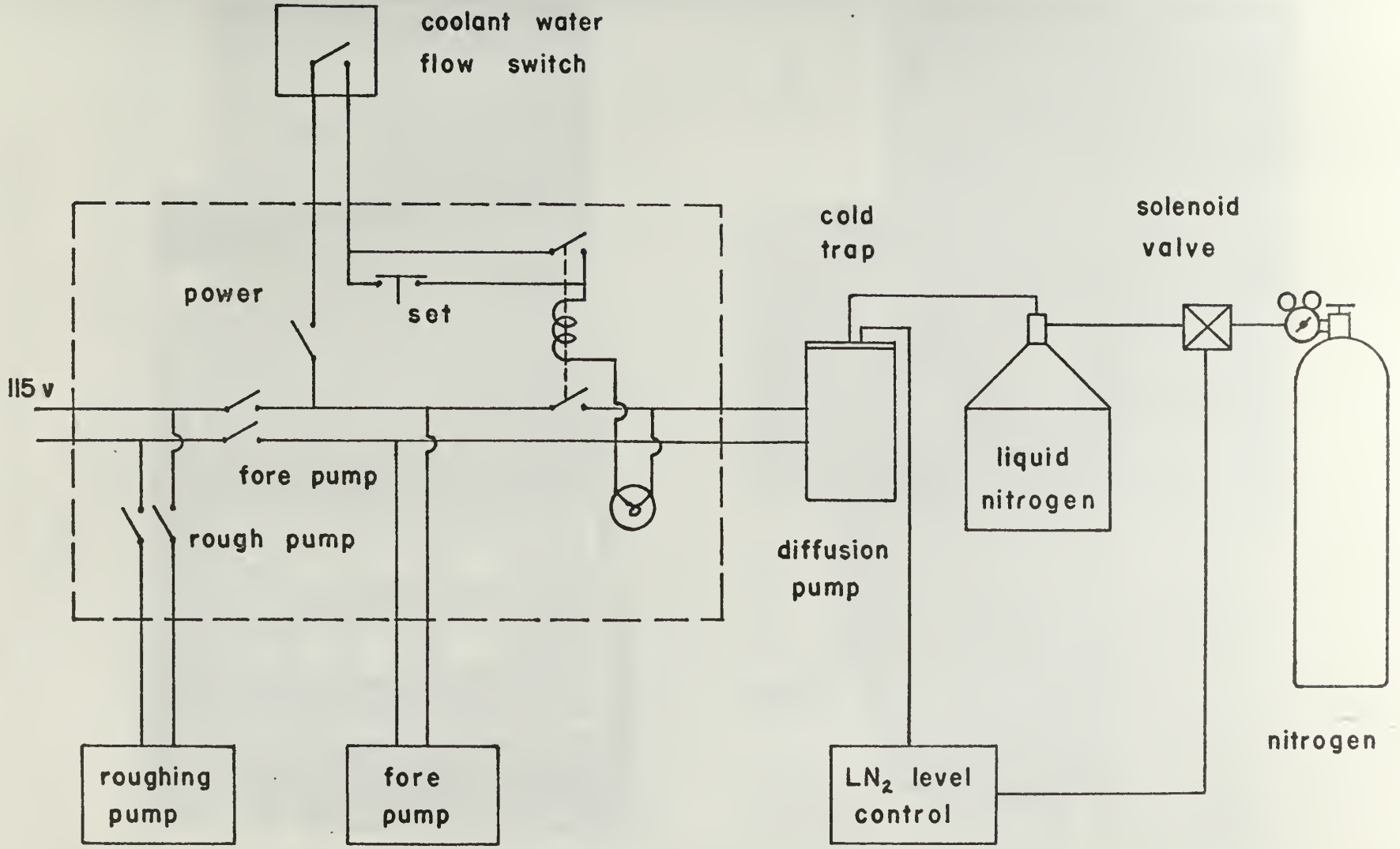
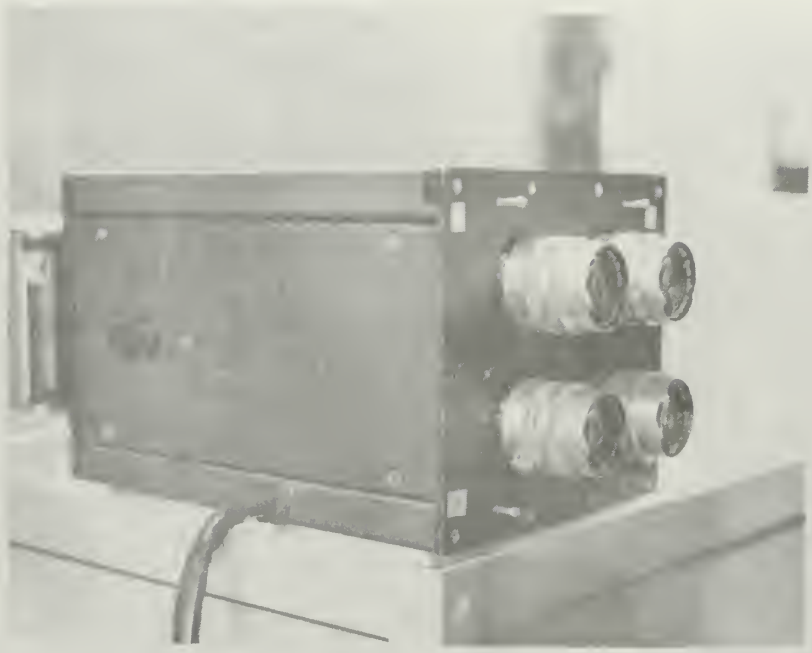


FIGURE 16 VACUUM CONTROLS



17 A

CAMERA

HEAD



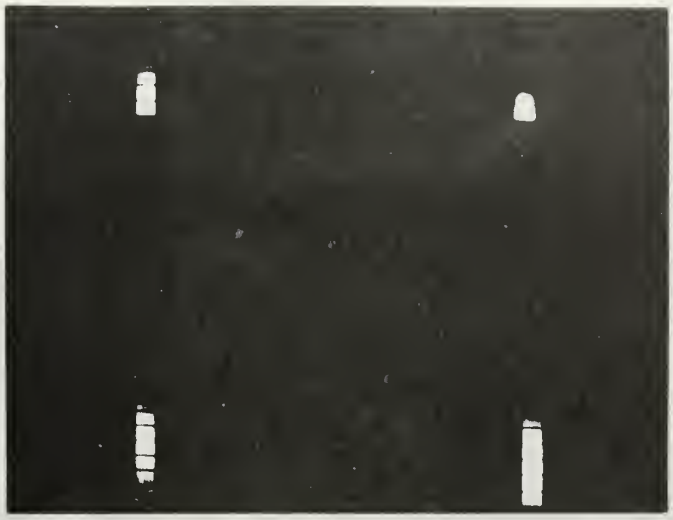
17 B

CAMERA

CONTROL

FIGURE 17

IMAGE CONVERTER CAMERA

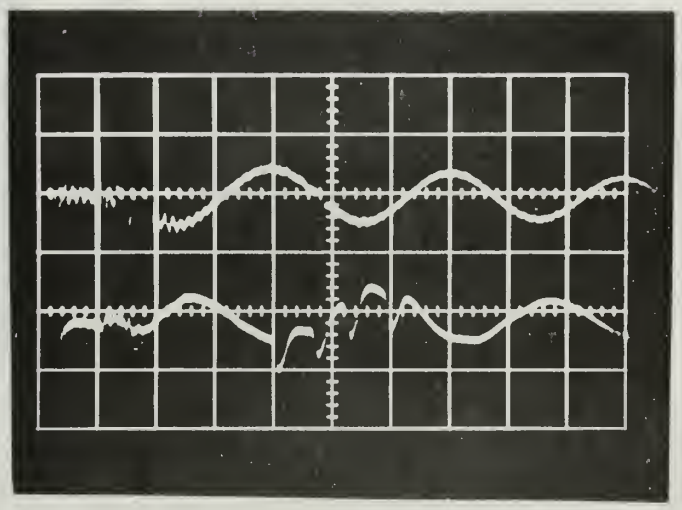


exposure time

.1 microsecond

FIGURE 18 A

IMAGE CONVERTER RECORD



upper - $\frac{dI}{dt}$

lower - camera monitor

scales:

time - 2 μs/cm

upper - .5 v/cm

lower - 10 v/cm

FIGURE 18 B

OSCILLOSCOPE RECORD



FIGURE 19

APPARATUS PLACEMENT



FIGURE 20 SAMPLE REMOVAL

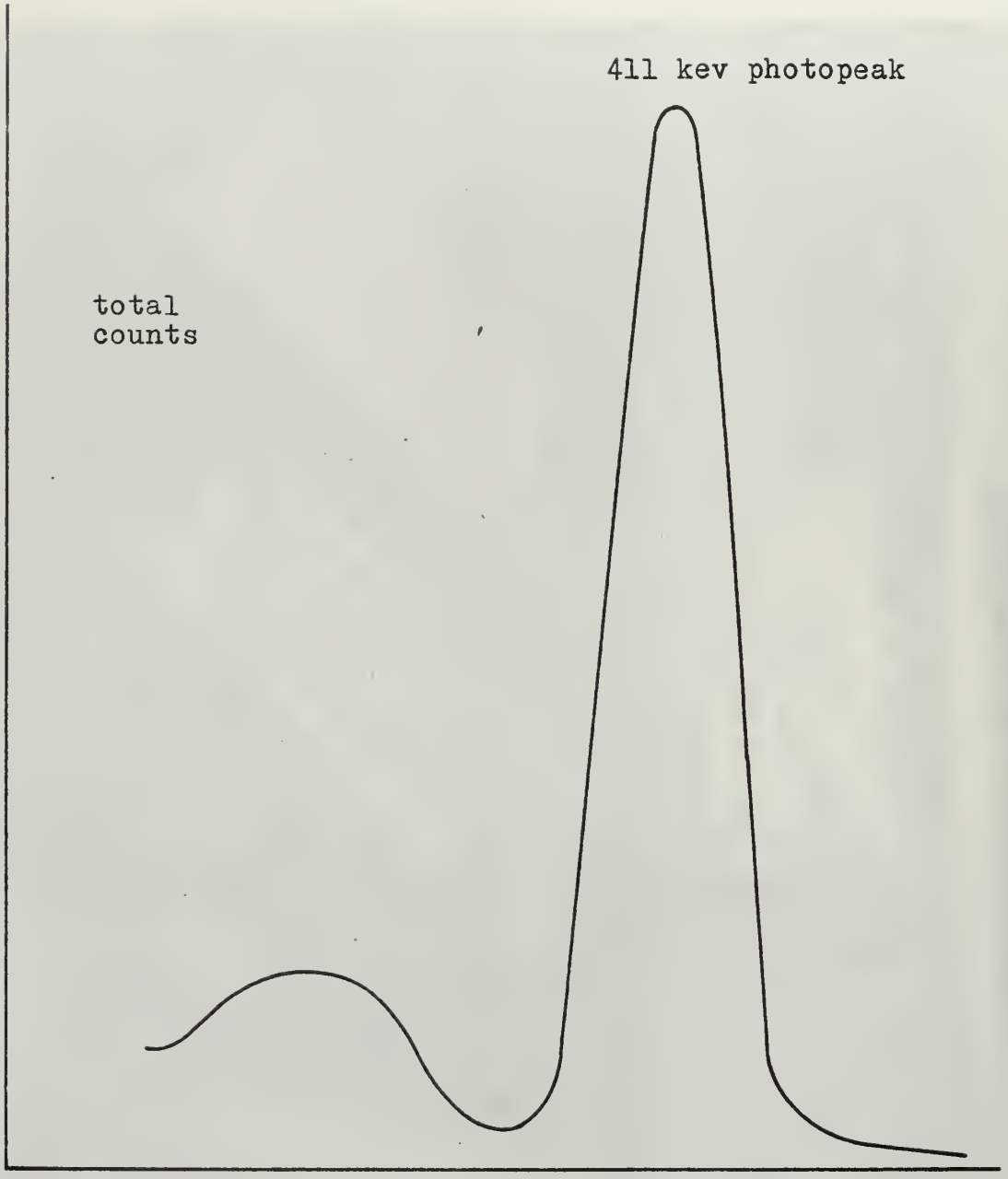


Figure 21 Gold 198 Gamma Radiation

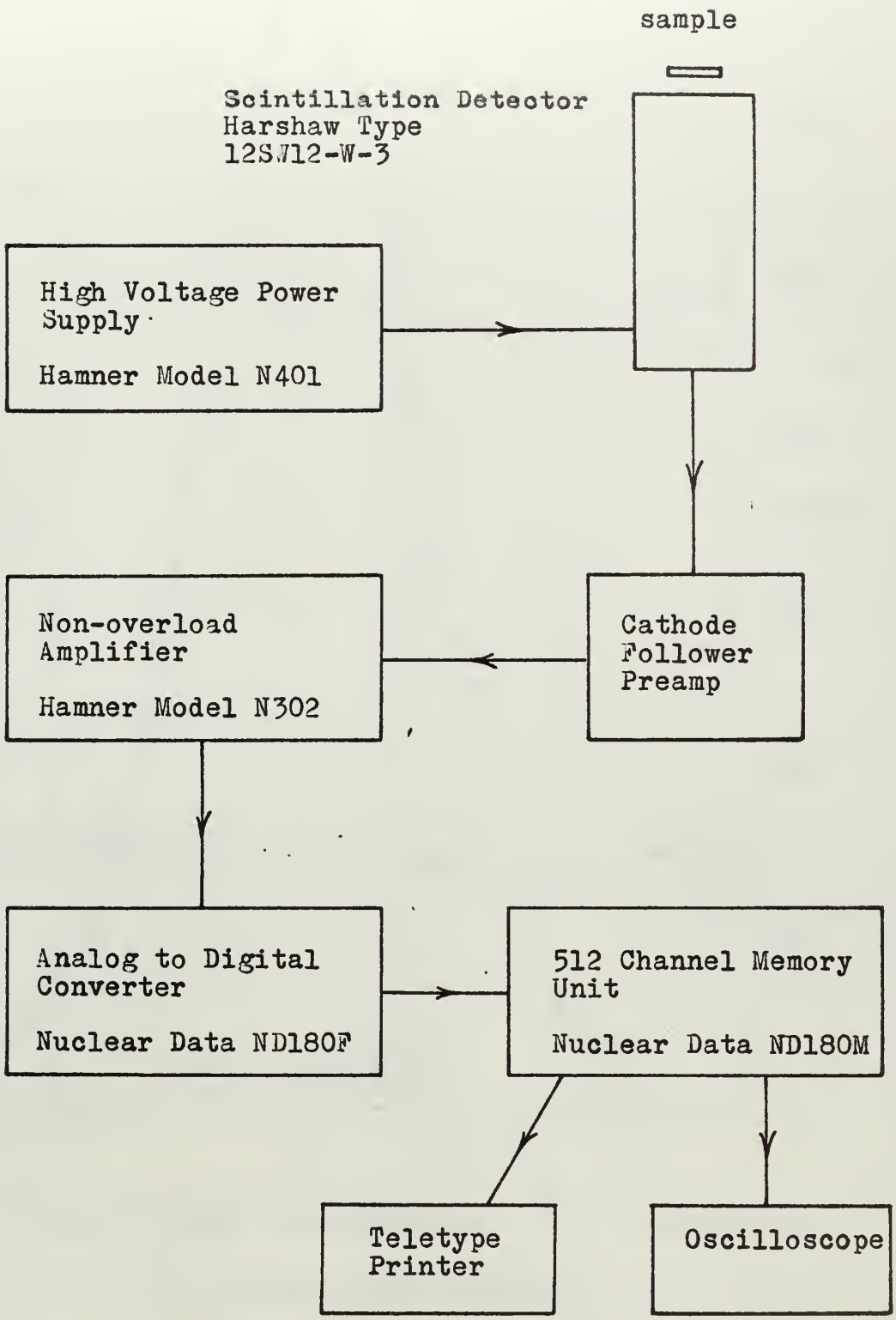
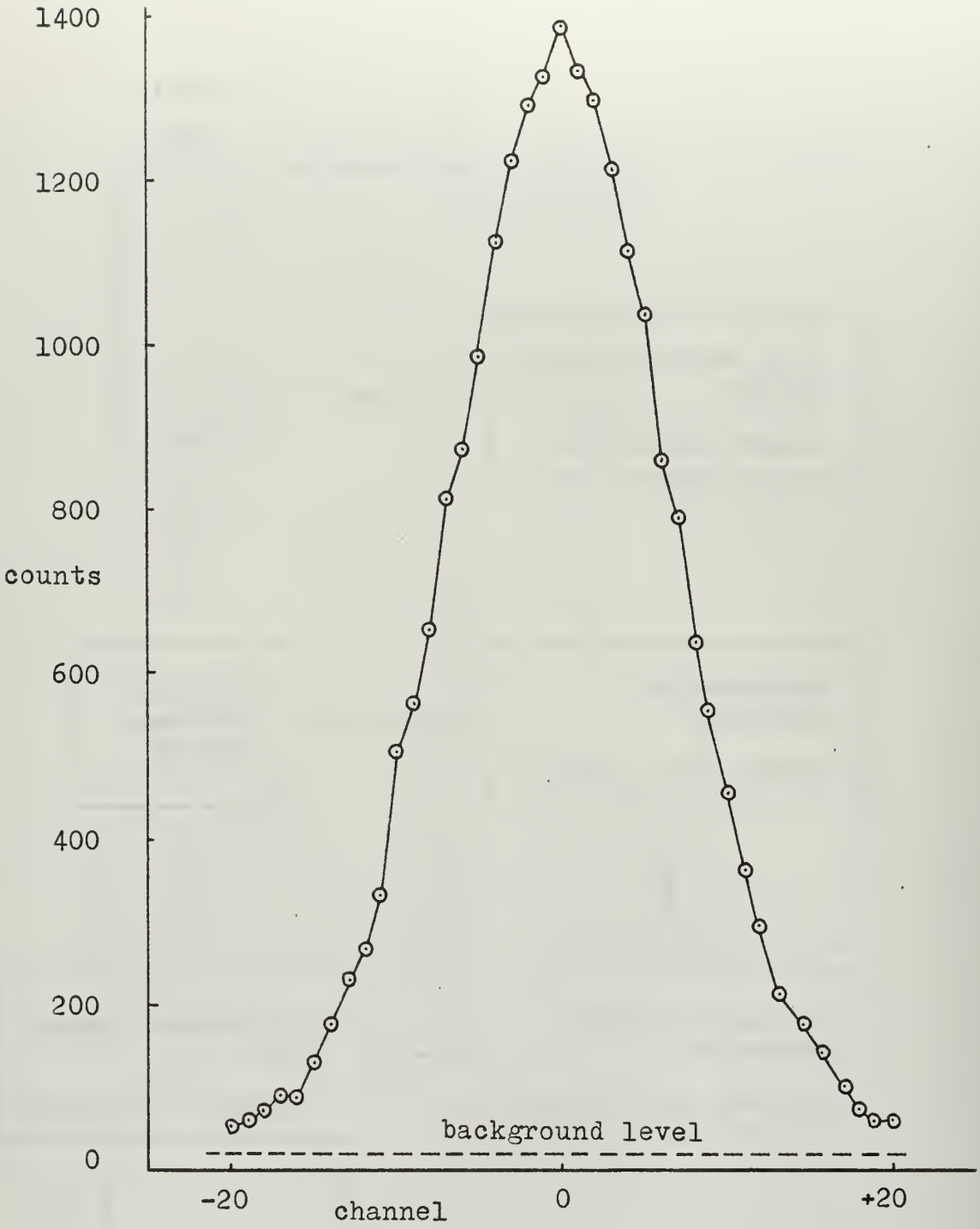


Figure 22 Detection Apparatus



Sample: 19L-9 Counted: 15 Mar 1227 Age: 19.6 hr

Count time: 10 min Area: 11.28 in^2

Figure 23 Sample Data Plot

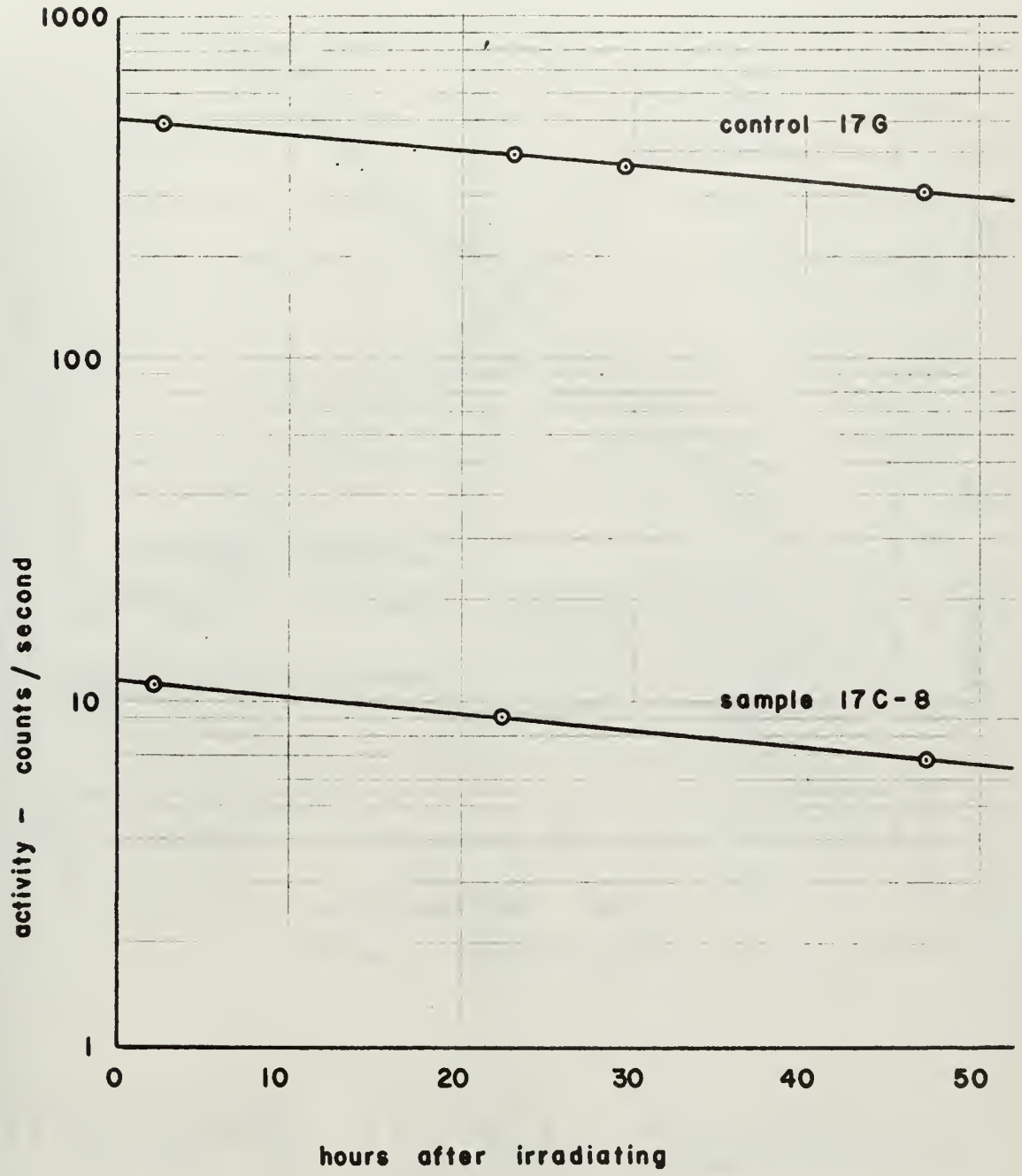


FIGURE 24 GOLD DECAY

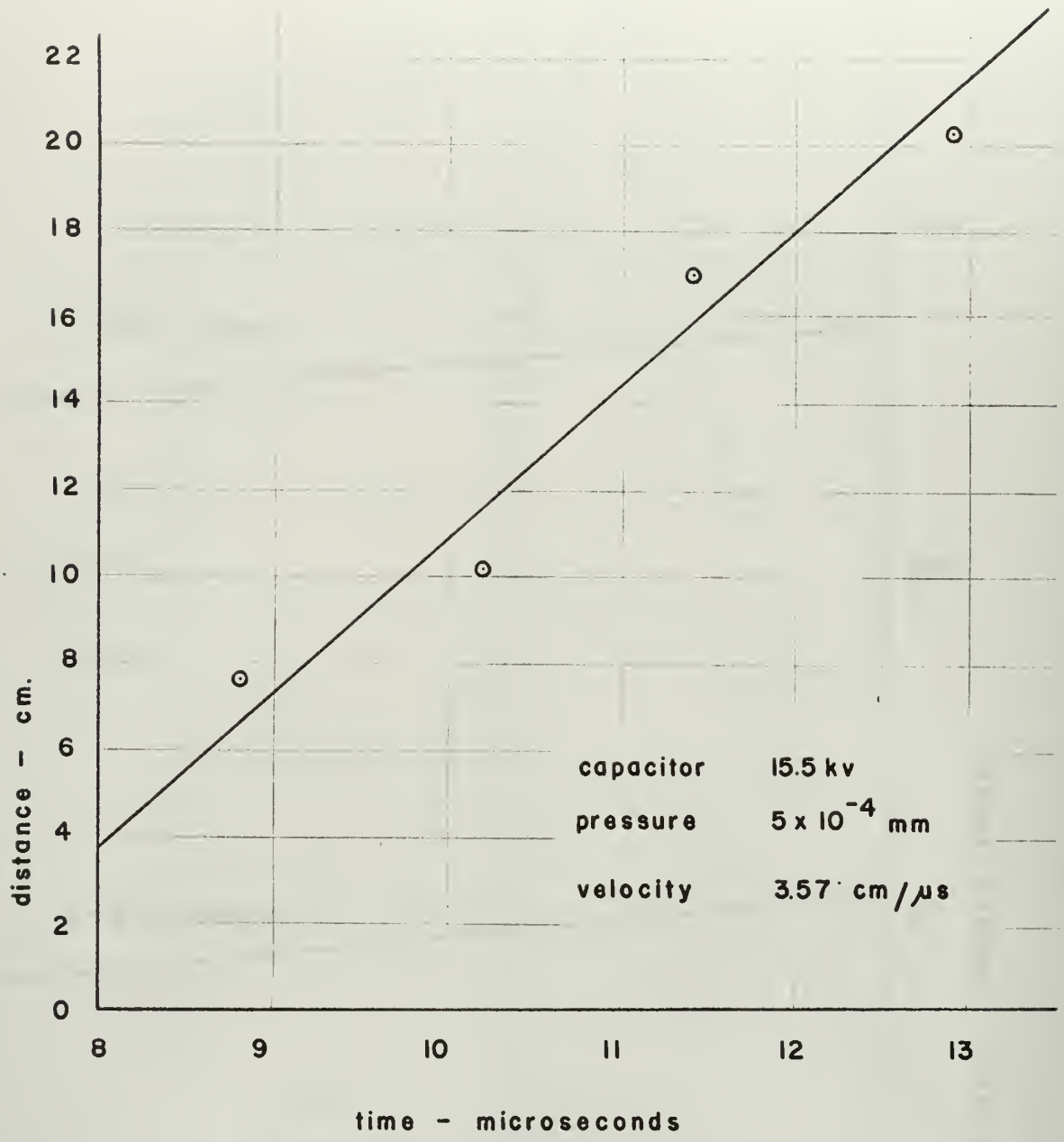


FIGURE 25 VELOCITY MEASUREMENT

SHOT 11

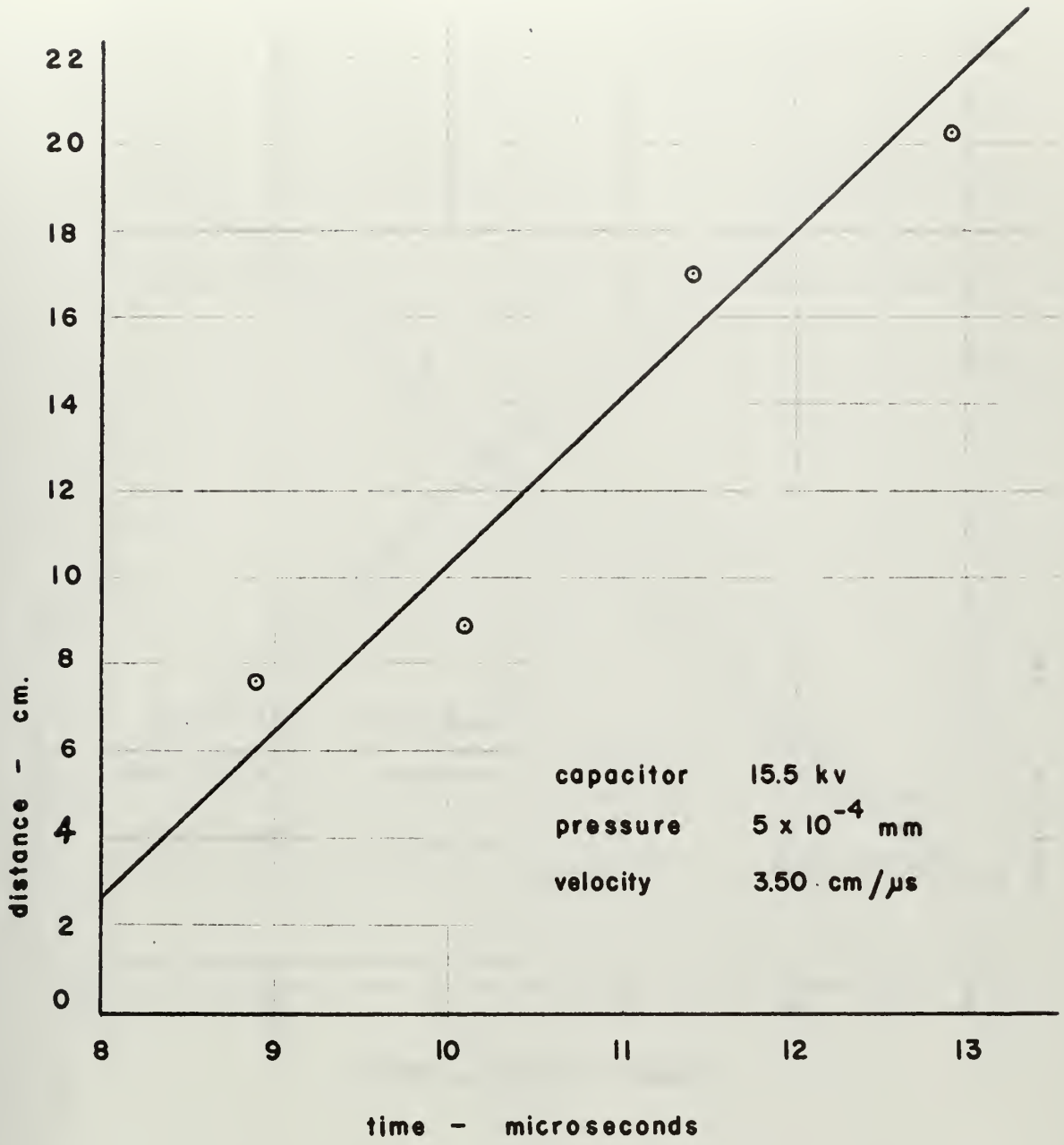


FIGURE 26 VELOCITY MEASUREMENT
SHOT 12

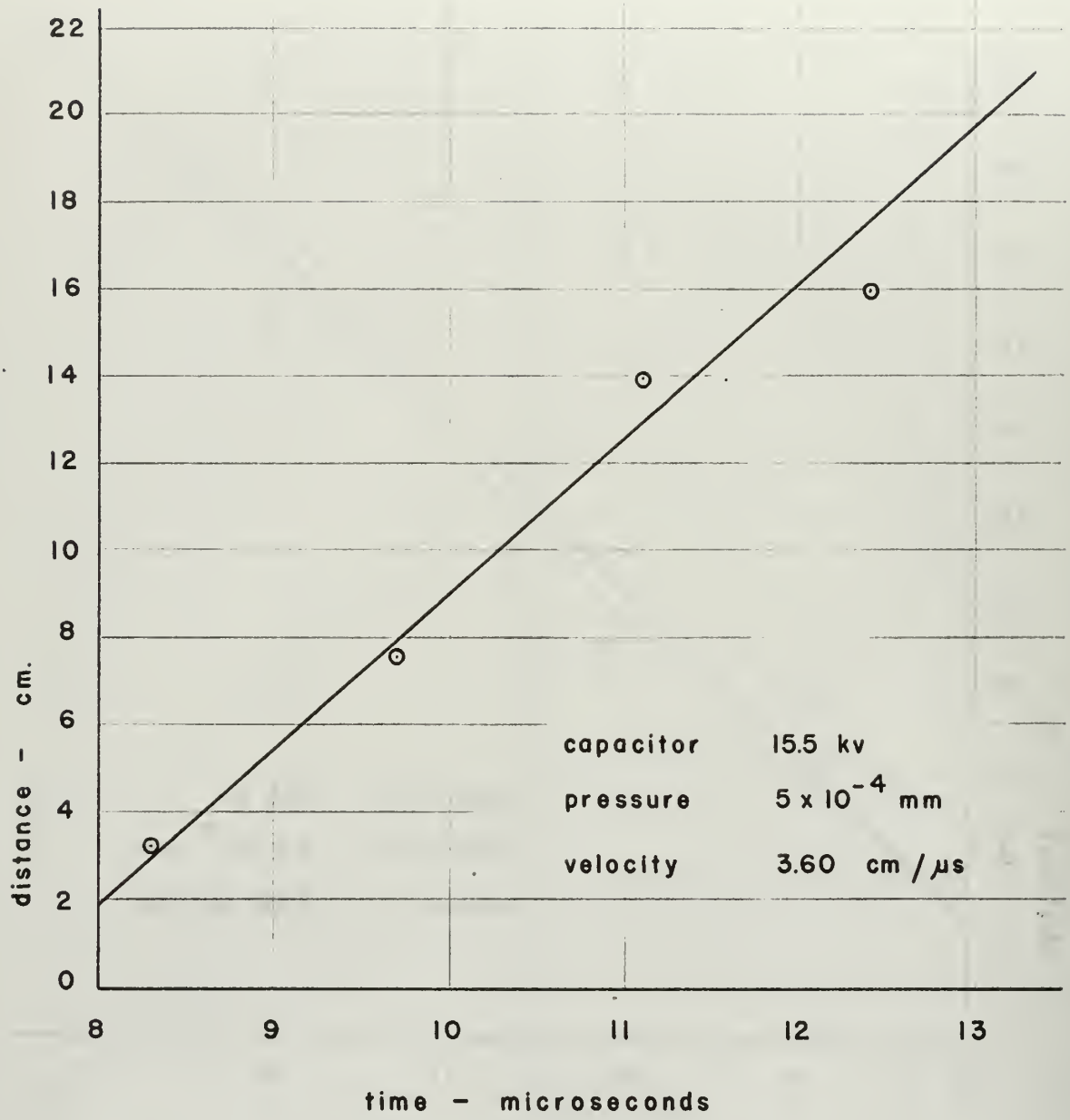


FIGURE 27 VELOCITY MEASUREMENT
SHOT 13

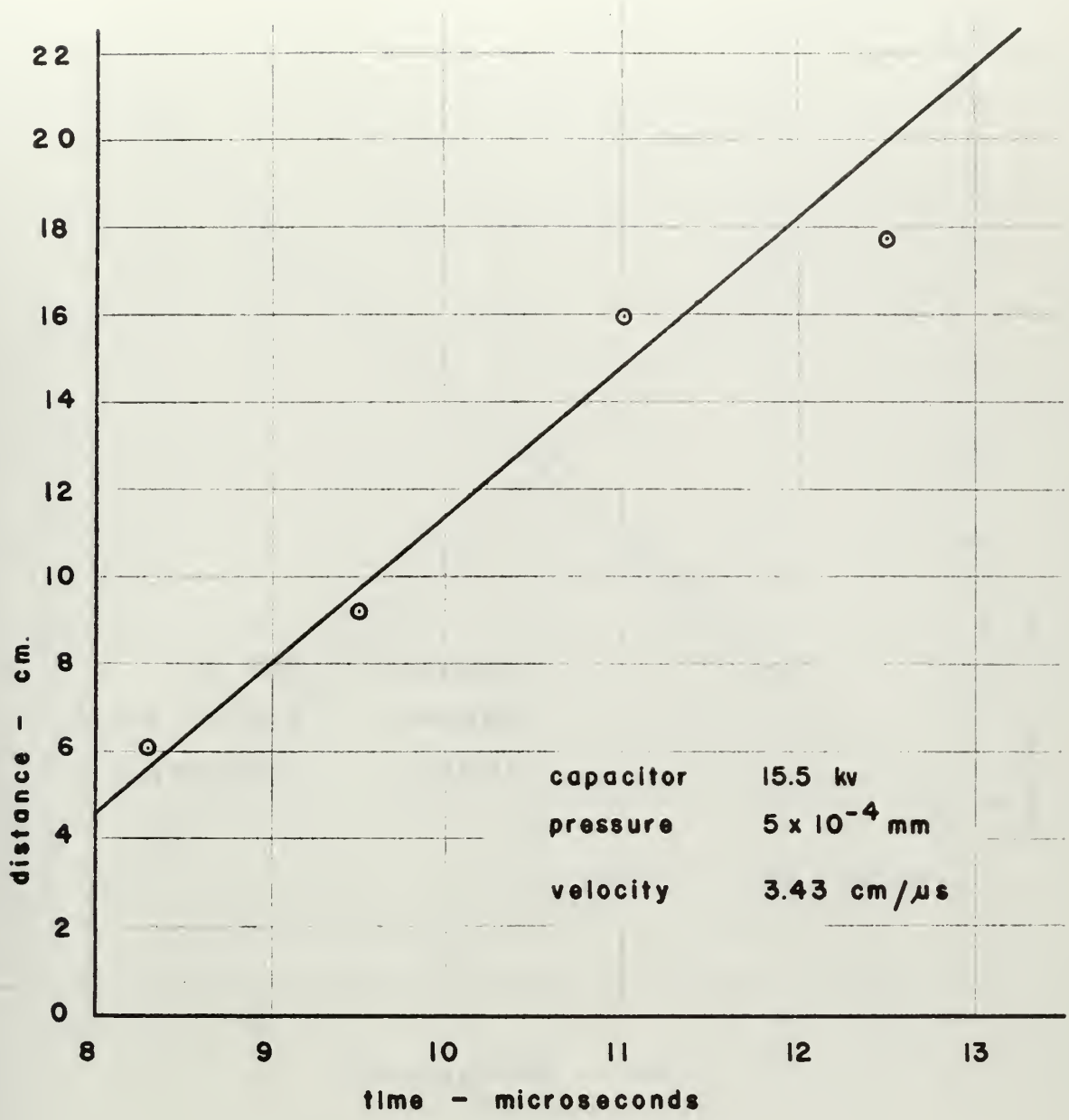


FIGURE 28 VELOCITY MEASUREMENT

SHOT 14

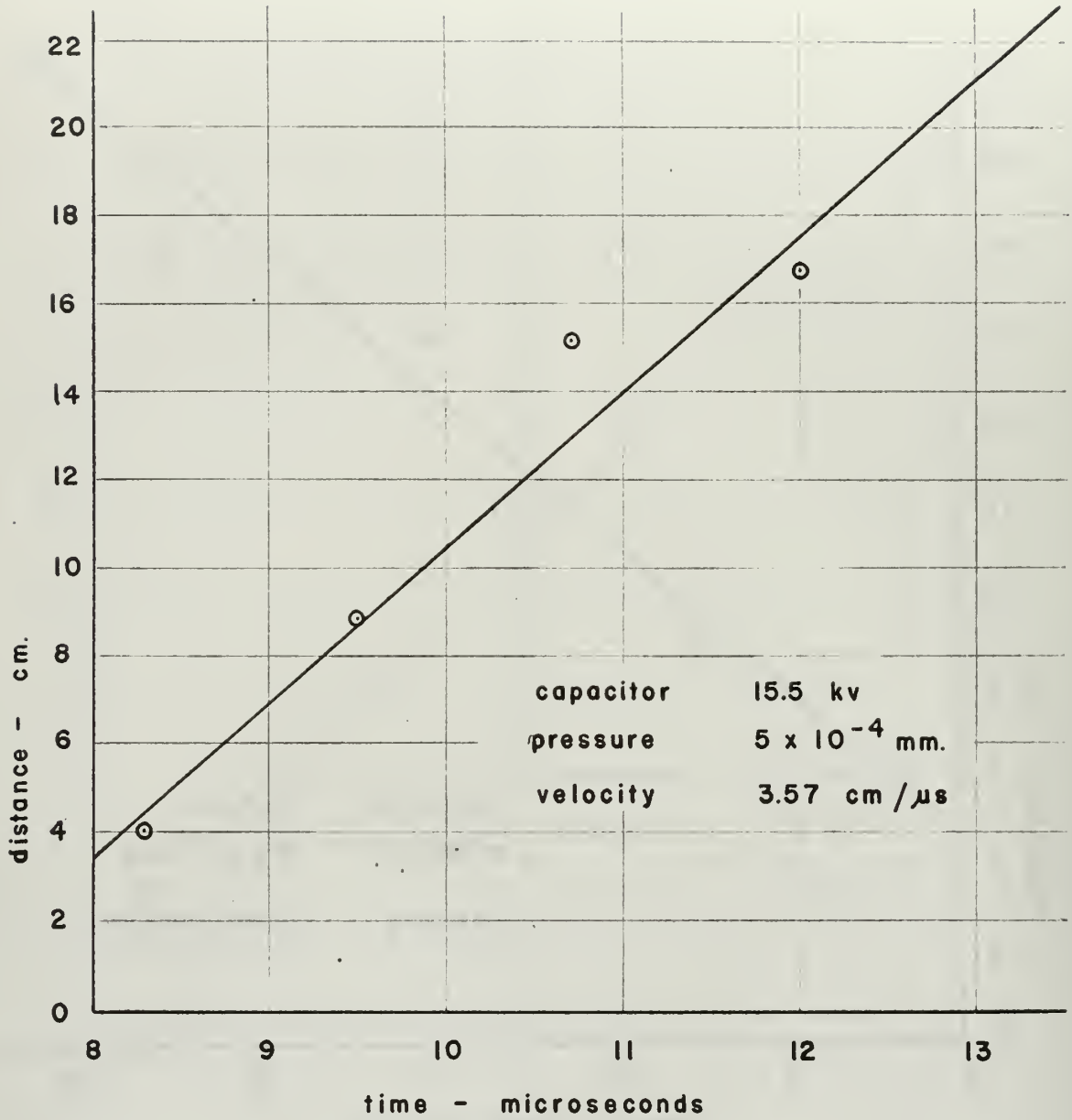


FIGURE 29 VELOCITY MEASUREMENT
SHOT 16

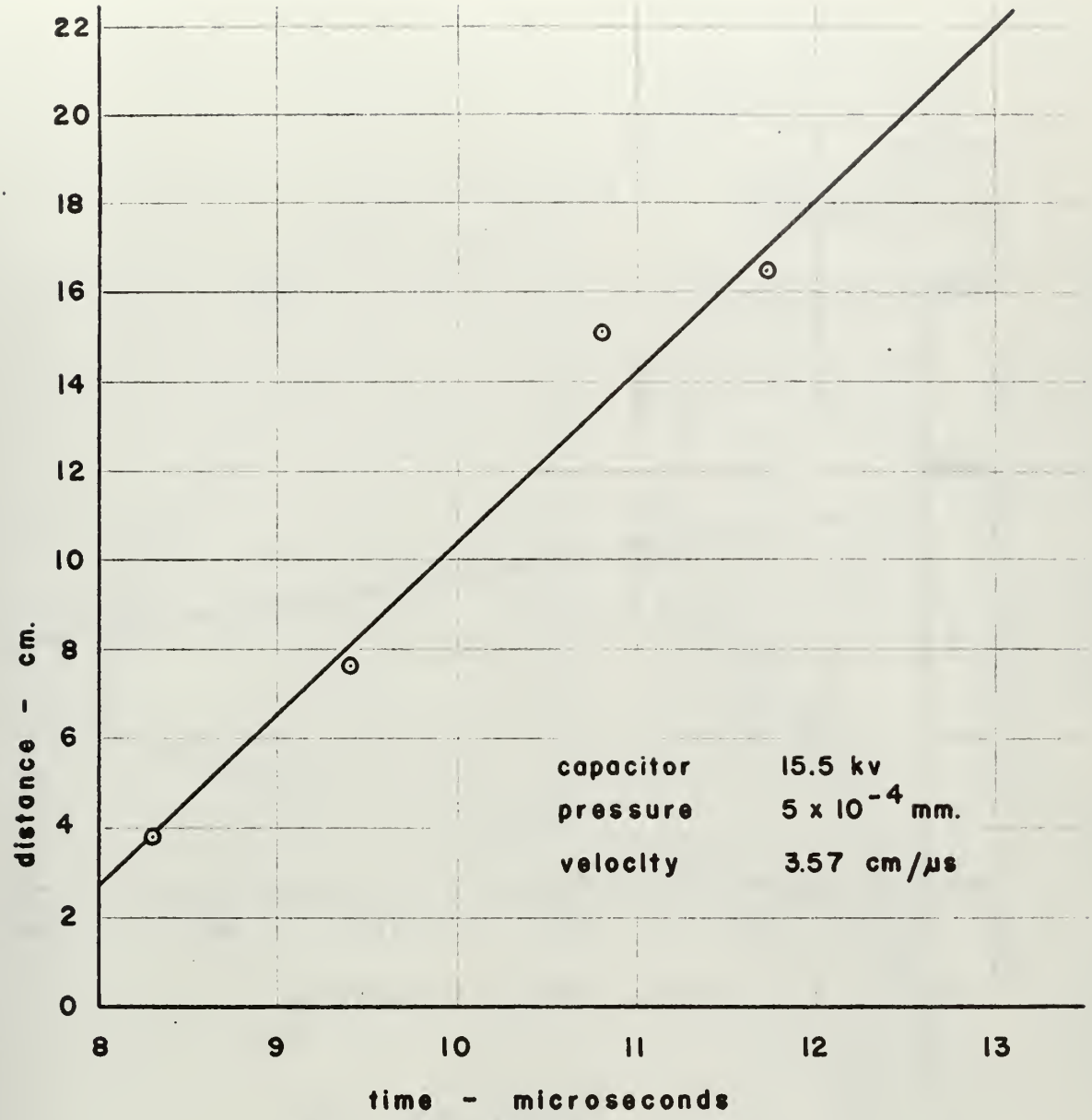


FIGURE 30 VELOCITY MEASUREMENT
SHOT 18

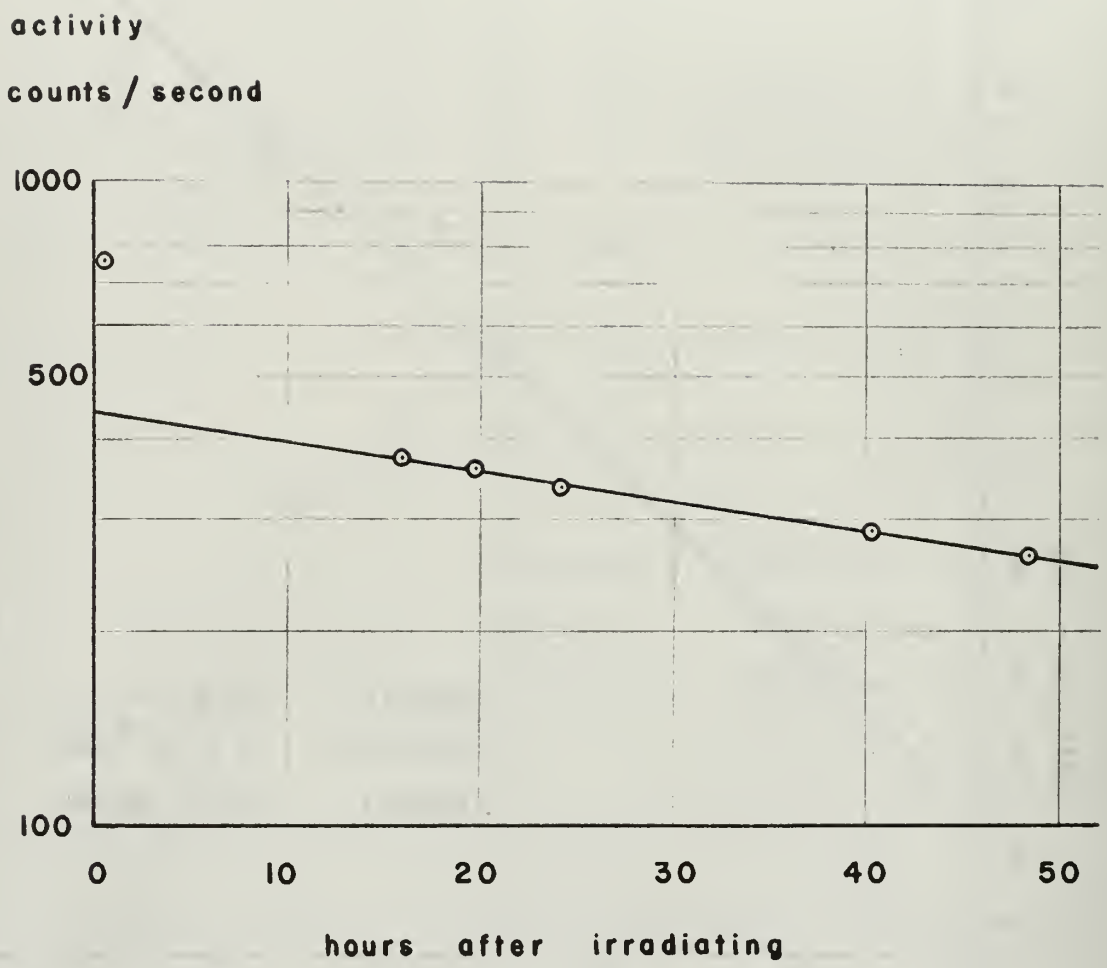


FIGURE 31

GOLD MONITOR DECAY

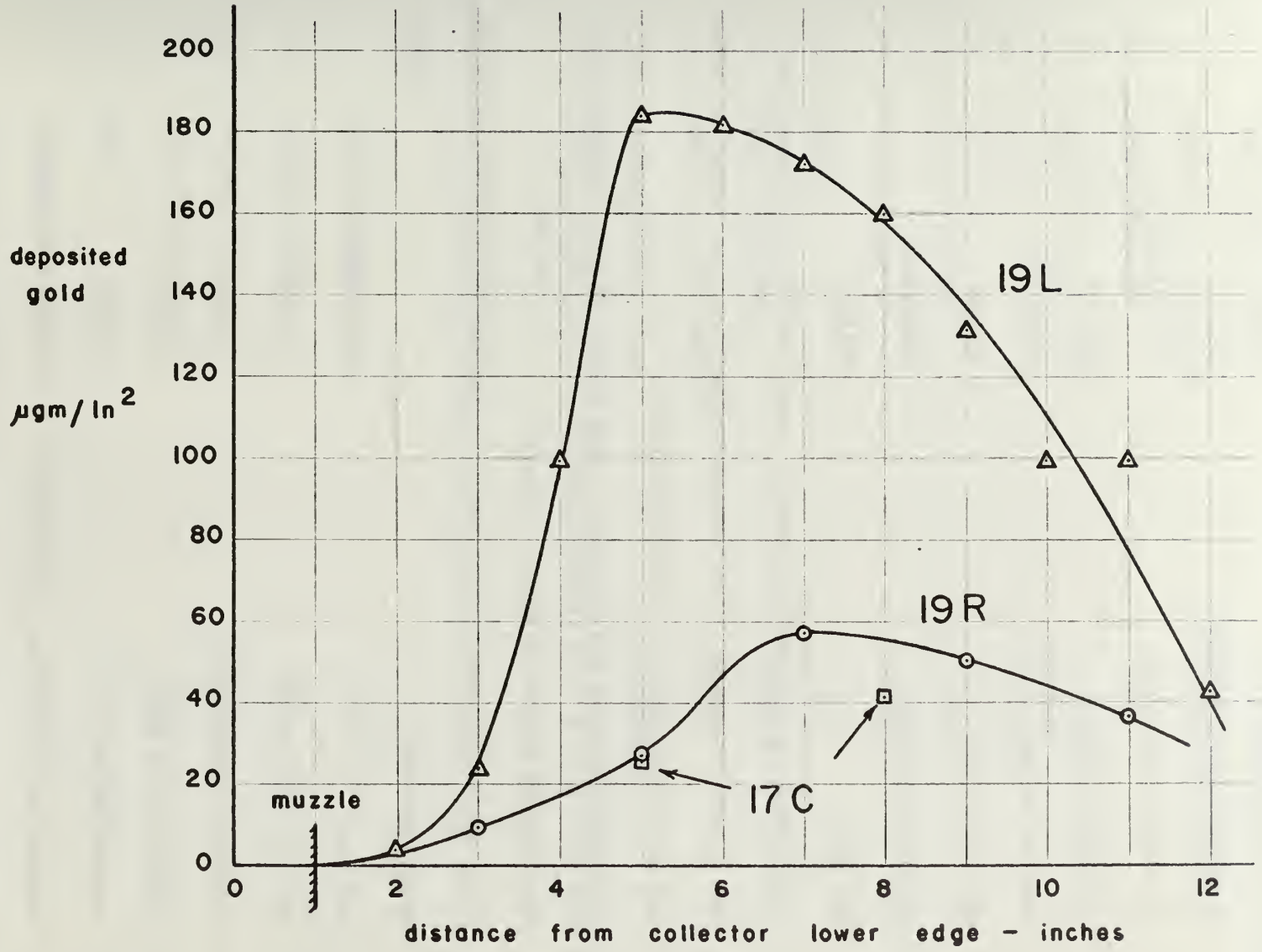


FIGURE 32 GOLD DEPOSITION

APPENDIX I

PROCEDURES CHECKLISTS

PREPARATION FOR FIRING

1.	Capacitor power master	OFF
2.	Capacitor ground rod	INSTALLED
3.	Ionization gage	OFF
4.	Vacuum valves 1 and 2	CLOSED
5.	Vacuum system	START
6.	Bell jar vent valve	OPENED
7.	Bell jar	RAISED

8. Disassemble and clean gun barrels, base, collecting cylinder and bell jar with acetone. Use suction device to remove particles inside gun and around base of vacuum manifold.

9. Assemble gun with foil in place, holes facing camera. Inspect foil from muzzle end for wrinkles or tears.

10. Place collector sheet in cylinder and slip over gun barrel with opening facing camera.

11.	Bell jar	LOWERED
12.	Bell jar vent valve	CLOSED
13.	Ionization gage valve	OPENED
14.	Thermocouple gage	ON #2
15.	Vacuum valve 2	OPEN
16.	Vacuum valves (below 10 microns)	OPEN 1, CLOSE 2
17.	Ionization gage (below 1 micron)	OPERATE

When desired vacuum is reached:

FIRING

1.	Ignitron pulser	ON
2.	Pulser power supply	ON, SET 3 KV
3.	Cameras/oscilloscope	READY
4.	Ionization gage	OFF
5.	Ionization gage valve	CLOSE
6.	Capacitor	CHARGE
7.	Camera shutters	OPEN
8.	Vacuum valve 1	CLOSE
9.	Trigger	FIRE
10.	Camera shutters	CLOSE
11.	Capacitor power master	OFF
12.	Capacitor ground rod	INSTALL

NOTE: Step 9 must be performed rapidly after 8 to prevent loss of vacuum.

VACUUM SYSTEM OPERATION

START

1.	Vacuum valves 1 and 2	CLOSE
2.	Roughing pump	ON
3.	Fore pump	ON
4.	Thermocouple gage	ON #1
5.	Water	ON $\frac{1}{4}$ TURN
6.	Diffusion pump (below 500 microns)	ON, SET
7.	Ionization gage (below 1 micron)	ON

SECURE

1.	Ionization gage	OFF
2.	Diffusion pump	OFF
3.	Roughing pump	OFF
4.	Fore pump	OFF
5.	Thermocouple gage	OFF
6.	Water (after 15 minutes)	OFF

IMAGE CONVERTER CAMERA OPERATION

READY

1.	Camera power	ON
2.	Lens covers	REMOVE
3.	Lenses	FOCUS
4.	Focus ports	CLOSE
5.	Delays	SET
6.	Exposure times	SET
7.	Polaroid film remaining	CHECK

CAPACITOR POWER CONTROL

EMERGENCY

1.	Master	OFF/ABORT
2.	Capacitor ground rod	INSTALLED

SAFETY/ABORT

Same as emergency. System should be in this condition whenever working near capacitor.

CAPACITOR CHARGE

1.	Switches	OFF, CCW
2.	Capacitor ground rod	REMOVED
3.	Master	ON/ISOLATE
4.	Charge switch	CHARGE
5.	Filament control	OPERATE
6.	Voltage control	SET

NOTE: Do not set above 30 kv on voltage control dial.
Do not exceed 20 kv capacitor voltage. (Read with Voltage Control OFF)

When desired Capacitor Voltage is reached:

7.	Voltage control	OFF
8.	Filament control	OFF
9.	Charge switch	ISOLATE

Capacitor is now ready to fire.

APPENDIX II

CAPACITOR VOLTMETER CALIBRATION

To insure reproducibility and uniformity of the plasma gun discharge it is necessary to measure capacitor voltage accurately. The charging power supply was originally equipped with a voltmeter which indicated driving voltage while charging only. For accurate determination of capacitor power level a voltmeter directly across the capacitor was required. To keep power dissipation losses through the meter to a minimum, a large resistor in series with the most sensitive meter available would be desirable.

A maximum discharge voltage of 15.5 kv was set as an upper limit to avoid capacitor damage from an excessively large voltage reversal. Since an ammeter requiring 50 microamps for full scale deflection was available, a resistor giving roughly one half scale deflection at 15 kv was fabricated for use in series.

The high voltage series resistor was fabricated using forty 15 megohm resistors in series mounted on a phenolic sheet inside the power supply cabinet. A 100 kv meter was then obtained and connected directly across the capacitor to calibrate the microammeter.

For calibration runs the capacitor was charged to maximum voltage, then the charging voltage removed and the stored energy allowed to bleed through the microammeter circuit to ground. As capacitor voltage fell, the microammeter reading and the actual voltage were recorded. Two complete runs produced identical values which are given in Table II-I. The resulting

calibration curve is given in Fig. II-1. A copy of this curve was attached to the power supply.

For the initial run a capacitor voltage of 25 kv was used but ignitron breakdown occurred shortly after charging. Data points were obtained for voltages to 24 kv but the ignitron breakdown point occurred at successively lower voltages for the two following runs. It is recommended that 20 kv not be exceeded since this is the ignitron rating and breakdown due to overvoltage appears to cause a deterioration in the ability of the ignitron to resist breakdown.

TABLE II-I

VOLTMETER CALIBRATION

1. High volt meter directly across capacitor - kilovolts

2. 50 μamp meter in series with 600 megohms

1.	2.	1.	2.
24.0	.950	15.5	.700
23.5	.930	15.0	.685
23.0	.920	14.5	.665
22.5	.900	14.0	.655
22.0	.880	13.5	.630
21.5	.860	13.0	.620
21.0	.845	12.5	.595
20.5	.835	12.0	.585
20.0	.825	11.5	.575
19.5	.805	11.0	.565
19.0	.795	10.5	.550
18.5	.775	10.0	.535
18.0	.770	8.0	.475
17.5	.760	6.0	.395
17.0	.750		
16.5	.735		
16.0	.720		

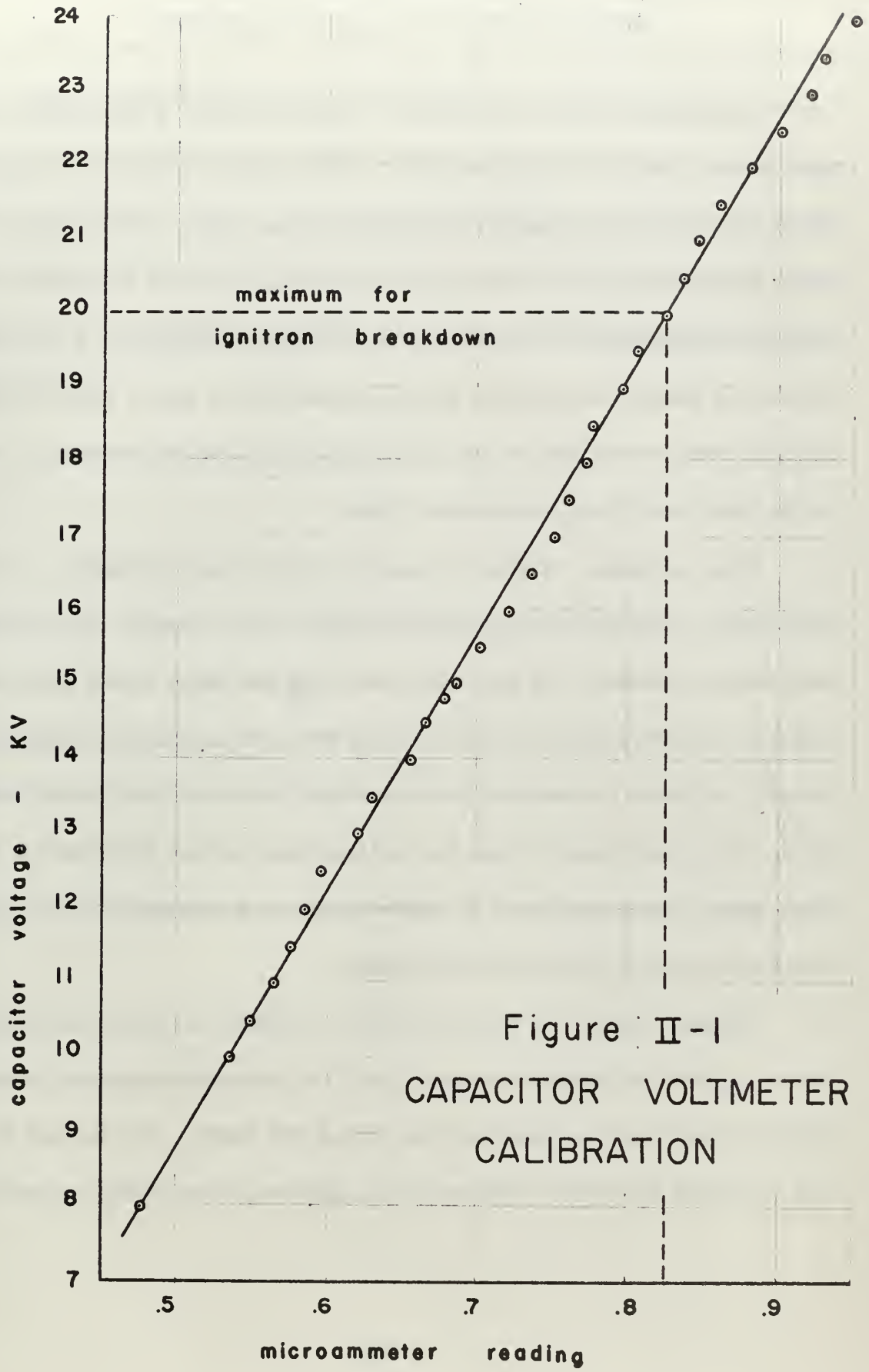


Figure II-1

CAPACITOR VOLTMETER CALIBRATION

APPENDIX III

IMAGE CONVERTER CAMERA CALIBRATION

1. Triggering. Since the Abtronics camera requires a signal with a rise time of the order of .1 microsecond it was originally planned to trigger this camera utilizing the capacitor discharge trigger pulse. It was found, however, that the balance of the trigger circuit was upset by this additional load and consequently it would not fire the pulser thyratron. A simple device which was found to trigger the camera satisfactorily was a single loop of stranded wire wound around one of the ignitron pulse transformers. This method was used for all subsequent tests.

2. Delay settings. Since the plasma velocity was not known, a few runs were made to determine the necessary delay time to "catch" the plasma front with the camera. It was also found that the delay times were more uniform from one shot to the next if only the first shutter was triggered externally and each succeeding shutter delayed from the last channel which fired. Since the delay setting dial calibrations are not accurate for short delay times, the actual time of shutter firing was obtained from an oscilloscope trace of the camera monitor output.

3. Exposure times. It was found that, although the image brightness decreases with shortened exposure time, the minimum exposure time of .1 microseconds could be used without losing the image. The fastest Polaroid film available (type 410, ASA speed 10,000) was used in the recording camera.

4. Lens Settings. Initial tests showed two of the images to be much brighter than the other two due to differences in either circuitry or the shutter tubes. Since image brightness is used in comparisons to determine plasma velocity it is imperative that all four images appear the same for the same light input. It was found that if lenses 1 and 2 were closed down to f/2.0 while lenses 3 and 4 were fully open (f/1.5), all four images were of equal intensity and sufficient light was still available to use the minimum exposure time of .1 microsecond.

APPENDIX IV

PREPARATION OF CONTROL SAMPLE DISK

In order to simplify determination of the amount of gold deposited on each sample disk, a control disk with a known weight of gold was prepared and used to determine unknown weights by direct comparison. This eliminated the need to observe the decay of each of the many samples over a long period of time. The decay of this control disk was monitored closely over a period of several days after irradiation.

The control sample was required to have as little gold mass as possible to avoid self-shielding effects when irradiated. Electroscope gold foils four microinches thick were used for this purpose. This foil was extremely fragile and could be handled only between sheets of paper. The weights of these foils were obtained by weighing a measured area on an electronic balance. The control sample was then prepared by spraying a coat of lacquer on one of the aluminum collector sheets and carefully laying the foil on the wet lacquer. When dry, the top surface of the gold was given another protective spray coat of lacquer. Control disks were then cut from this sheet using the sample cutting punch.

INITIAL DISTRIBUTION LIST

		No. Copies
1.	Defense Documentation Center Cameron Station Alexandria, Virginia 22314	20
2.	Library U. S. Naval Postgraduate School Monterey, California	2
3.	Commander, Naval Air Systems Command Department of the Navy Washington, D. C. 20360	1
4.	Chairman, Department of Aeronautics U. S. Naval Postgraduate School Monterey, California	2
5.	Prof. R. E. Reichenbach Department of Aeronautics U. S. Naval Postgraduate School Monterey, California	5
6.	LT Robert K. Brumwell, USN Box 1601 U. S. Naval Postgraduate School Monterey, California 93940	1

DOCUMENT CONTROL DATA - R&D

(Security classification of title, body of abstract and indexing annotation must be entered when the overall report is classified)

1. ORIGINATING ACTIVITY *(Corporate author)*
U. S. Naval Postgraduate School
Monterey, California

2a. REPORT SECURITY CLASSIFICATION
UNCLASSIFIED

2b. GROUP

3. REPORT TITLE

RADIOISOTOPE TRACING OF METALLIC DEPOSITS NEAR A COAXIAL PLASMA GUN EXHAUST

4. DESCRIPTIVE NOTES *(Type of report and inclusive dates)*
Aeronautical Engineer Thesis

5. AUTHOR(S) *(Last name, first name, initial)*
Brumwell, Robert K.

6. REPORT DATE	7a. TOTAL NO. OF PAGES	7b. NO. OF REFS
May 1966	87	22

8a. CONTRACT OR GRANT NO.	9a. ORIGINATOR'S REPORT NUMBER(S)
b. PROJECT NO.	
c.	9b. OTHER REPORT NO(S) *(Any other numbers that may be assigned this report)*
d.	

10. AVAILABILITY/LIMITATION NOTICES
This document has been approved for public release and sale; its distribution is unlimited.
Qualified requesters may obtain copies of this report from DDC
Merrubun 11/25/69

11. SUPPLEMENTARY NOTES	12. SPONSORING MILITARY ACTIVITY
	Commander, Naval Air Systems Command Department of the Navy, Washington, D.C.

13. ABSTRACT

A coaxial plasma accelerator system was constructed by LT R.K. Brumwell, USN at the United States Naval Postgraduate School for the purpose of producing a high velocity plasma slug. Experiments were performed in an evacuated chamber. Operating procedures were established for the apparatus and calibration tests were performed which demonstrated reproducibility of accelerator discharges made under given conditions.

Use of a radioisotope tracer technique to measure the deposition of a metallic plasma on a cold wall was then investigated. A series of tests was conducted which demonstrates the feasibility of this tracer method for determination of mass condensation on walls surrounding a high velocity plasma slug.

DD FORM 1 JAN 64 1473

14. KEY WORDS	LINK A		LINK B		LINK C	
	ROLE	WT	ROLE	WT	ROLE	WT
Plasma Plasma Accelerator Radioisotope Tracing of Plasma						

INSTRUCTIONS

1. ORIGINATING ACTIVITY: Enter the name and address of the contractor, subcontractor, grantee, Department of Defense activity or other organization *(corporate author)* issuing the report.

2*a*. REPORT SECURITY CLASSIFICATION: Enter the overall security classification of the report. Indicate whether "Restricted Data" is included. Marking is to be in accordance with appropriate security regulations.

2*b*. GROUP: Automatic downgrading is specified in DoD Directive 5200.10 and Armed Forces Industrial Manual. Enter the group number. Also, when applicable, show that optional markings have been used for Group 3 and Group 4 as authorized.

3. REPORT TITLE: Enter the complete report title in all capital letters. Titles in all cases should be unclassified. If a meaningful title cannot be selected without classification, show title classification in all capitals in parenthesis immediately following the title.

4. DESCRIPTIVE NOTES: If appropriate, enter the type of report, e.g., interim, progress, summary, annual, or final. Give the inclusive dates when a specific reporting period is covered.

5. AUTHOR(S): Enter the name(s) of author(s) as shown on or in the report. Enter last name, first name, middle initial. If military, show rank and branch of service. The name of the principal author is an absolute minimum requirement.

6. REPORT DATE: Enter the date of the report as day, month, year; or month, year. If more than one date appears on the report, use date of publication.

7*a*. TOTAL NUMBER OF PAGES: The total page count should follow normal pagination procedures, i.e., enter the number of pages containing information.

7*b*. NUMBER OF REFERENCES: Enter the total number of references cited in the report.

8*a*. CONTRACT OR GRANT NUMBER: If appropriate, enter the applicable number of the contract or grant under which the report was written.

8*b*, 8*c*, & 8*d*. PROJECT NUMBER: Enter the appropriate military department identification, such as project number, subproject number, system numbers, task number, etc.

9*a*. ORIGINATOR'S REPORT NUMBER(S): Enter the official report number by which the document will be identified and controlled by the originating activity. This number must be unique to this report.

9*b*. OTHER REPORT NUMBER(S): If the report has been assigned any other report numbers *(either by the originator or by the sponsor)*, also enter this number(s).

10. AVAILABILITY/LIMITATION NOTICES: Enter any limitations on further dissemination of the report, other than those imposed by security classification, using standard statements such as:

(1) "Qualified requesters may obtain copies of this report from DDC."

(2) "Foreign announcement and dissemination of this report by DDC is not authorized."

(3) "U. S. Government agencies may obtain copies of this report directly from DDC. Other qualified DDC users shall request through _____."

(4) "U. S. military agencies may obtain copies of this report directly from DDC. Other qualified users shall request through _____."

(5) "All distribution of this report is controlled. Qualified DDC users shall request through _____."

If the report has been furnished to the Office of Technical Services, Department of Commerce, for sale to the public, indicate this fact and enter the price, if known.

11. SUPPLEMENTARY NOTES: Use for additional explanatory notes.

12. SPONSORING MILITARY ACTIVITY: Enter the name of the departmental project office or laboratory sponsoring *(paying for)* the research and development. Include address.

13. ABSTRACT: Enter an abstract giving a brief and factual summary of the document indicative of the report, even though it may also appear elsewhere in the body of the technical report. If additional space is required, a continuation sheet shall be attached.

It is highly desirable that the abstract of classified reports be unclassified. Each paragraph of the abstract shall end with an indication of the military security classification of the information in the paragraph, represented as *(TS), (S), (C), or (U)*.

There is no limitation on the length of the abstract. However, the suggested length is from 150 to 225 words.

14. KEY WORDS: Key words are technically meaningful terms or short phrases that characterize a report and may be used as index entries for cataloging the report. Key words must be selected so that no security classification is required. Identifiers, such as equipment model designation, trade name, military project code name, geographic location, may be used as key words but will be followed by an indication of technical context. The assignment of links, roles, and weights is optional.

[redacted]

9 SEP 66
8 JUN 67
25 JUL 67
6 SEP 67
3 JUL 69

BINDERY
BINDERY
16253
17593
8759
S10003

Thesis
B82635
c.1

[redacted] 86544

Brumwell
Radioisotope tracing of metallic deposits near a coaxial plasma gun exhaust.

8 JUN 67
25 JUL 67
6 SEP 67
3 JUL 69

BINDERY
16253
17593
8759
S10003

86544

Thesis
B82635
c.1

Brumwell
Radioisotope tracing of metallic deposits near a coaxial plasma gun exhaust.

thesB82635
Radioisotope tracing of metallic deposit
3 2768 002 07835 4
DUDLEY KNOX LIBRARY